Chapter III:

Results & Discussion

"Seven Deadly Sins: Wealth without work, Pleasure without conscience, Science without humanity, Knowledge without character, Politics without principle, Commerce without morality, Worship without sacrifice." — Mahatma Gandhi

3. Results and discussion

As described in the previous chapter, we designed and synthesized three novel series of DPP-IV inhibitors, the first series was cyanopyrrolidine containing peptidomimetic based DPP-IV inhibitors, second series was peptidomimetic based DPP-IV inhibitors, devoid of CYP liabilities and third series was aminomethylpiperidone based DPP-IV inhibitors. All synthesized compounds were purified, characterized and subjected for *in-vitro* DPP-IV inhibition study to establish Structure Activity Relationship (SAR) of individual series. Selected short listed most potent compounds from each series were subjected for *in vitro* selectivity over related serine proteases. The most potent and selective compounds were further subjected for *in vivo* antidiabetic activity. Selected short listed compounds (most potent compounds : both *in vitro* & *in vivo*) were also subjected for PK studies.

In this section, we summarized results and discussion of :

a) Cyanopyrrolidine containing peptidomimetic based DPP-IV inhibitors (First series)

b) Peptidomimetic based DPP-IV inhibitors, devoid of CYP liabilities (Second series)

c) Aminomethylpiperidone based DPP-IV inhibitors (Third series), in following sections:

- Synthesis of three different series (Chemistry)
- *In vitro* DPP-IV inhibitory activity, selectivity and SAR
- *In vitro* CYP inhibition study
- *In vivo* (antidiabetic activity) evaluation of DPP-IV inhibitors
- PK studies of selected compounds
- Docking studies

3.1. Cyanopyrrolidine containing peptidomimetic based DPP-IV inhibitors (First series)

3.1.1. Chemistry

In the previous section rational for designing cyanopyrrolidine containing peptidomimetic based potent DPP-IV inhibitors has been described, wherein we intended to synthesize the compounds represented by general structures **11a-h**, **12a-h, 16a-h, 17a-d** and **18a-b** (**Figure 24**). Synthetic methodology was designed based on the retrosynthetic analysis and the schemes are described below. Synthetic method reported in literature were adapted for the synthesis of title compounds **11a-h**, **12a-h, 16a-h, 17a-d** and **18a-b** respectively. All compounds were synthesized following the procedure reported earlier in literature by choosing the appropriate starting materials and optimizing reaction conditions.

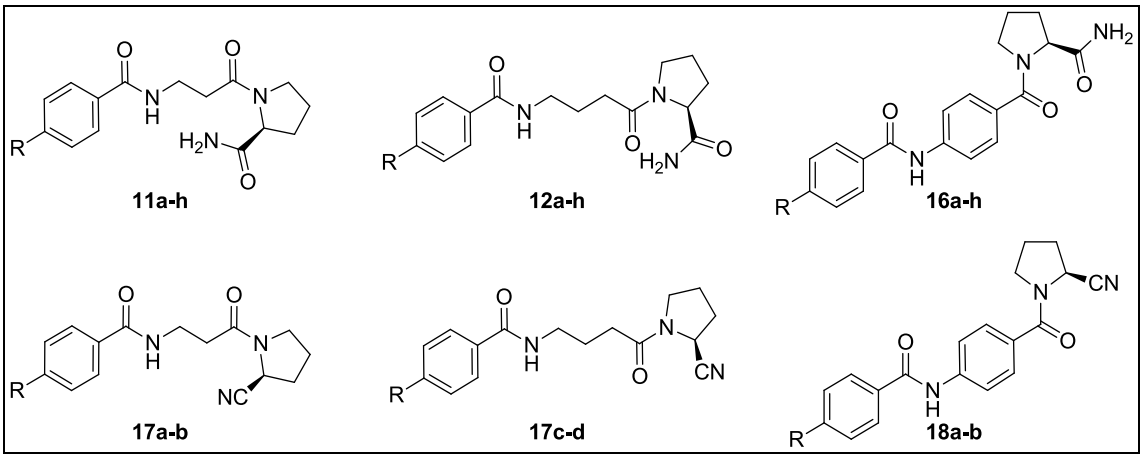

Figure 24. cyanopyrrolidine containing peptidomimetic based DPP-IV inhibitors

Synthesis of designed compounds **11a-h**, **12a-h, 16a-h, 17a-d** and **18a-b** is illustrated in **Schemes 1-3.** Novel peptidomimetics were synthesized using Fmoc-based Solid Phase Peptide Synthesis (SPPS) approach **[237]**, starting from commercially available Fmoc Rink Amide MBHA resin **1**. Deprotection of **1** with 20% piperidine in DMF and 1,3-diisopropylcarbodiimide (DIC) coupling with Fmoc-protected natural amino acid Proline **2** gives the resin-bouned Fmoc-protected amino acid **3**. Deprotection of **3** with 20% piperidine in DMF and DIC coupling with Fmoc protected unnatural aminoacids β-alanine (Fmoc-NH-$(CH_2)_2$-COOH) **4** , γ-amino butanoic acid (Fmoc-NH-$(CH_2)_3$-COOH) **5** or *p*-amino benzoic acid (PABA) **13** gives Fmoc-protected resin bound dipeptide **6**, **7** or **14** respectively. Deprotection of **6**, **7** and **14** with 20% piperidine in DMF and DIC

coupling with substituted benzoic acids **8a-h** gives fully-protected resin bounded peptoides **9a-h**, **10a-h** and **15a-h**. Final cleavage from resin was achieved by treatment with cleavage mixture of TFA, H_2O and Triisopropylsilane to give pyrrolidinecarboxamide based peptidomimetics **11a-h** ,**12a-h** and **16a-h**. Dehydration of pyrrolidinecarboxamide based peptidomimetics **11e-f**, **12e-f** and **16e-f** using trifluoroacetic anhydride at room temperature provided cyanopyrrolidin based peptidomimetics **17a-d** and **18a-b**.

Crude peptidomimetics thus obtained were purified using semi-preparative HPLC on a Shimadzu model LC-8A liquid chromatography. Desired fractions were pooled together, frozen and lyophilized to give title compounds **11a-h**, **12a-h, 16a-h, 17a-d** and **18a-b**.

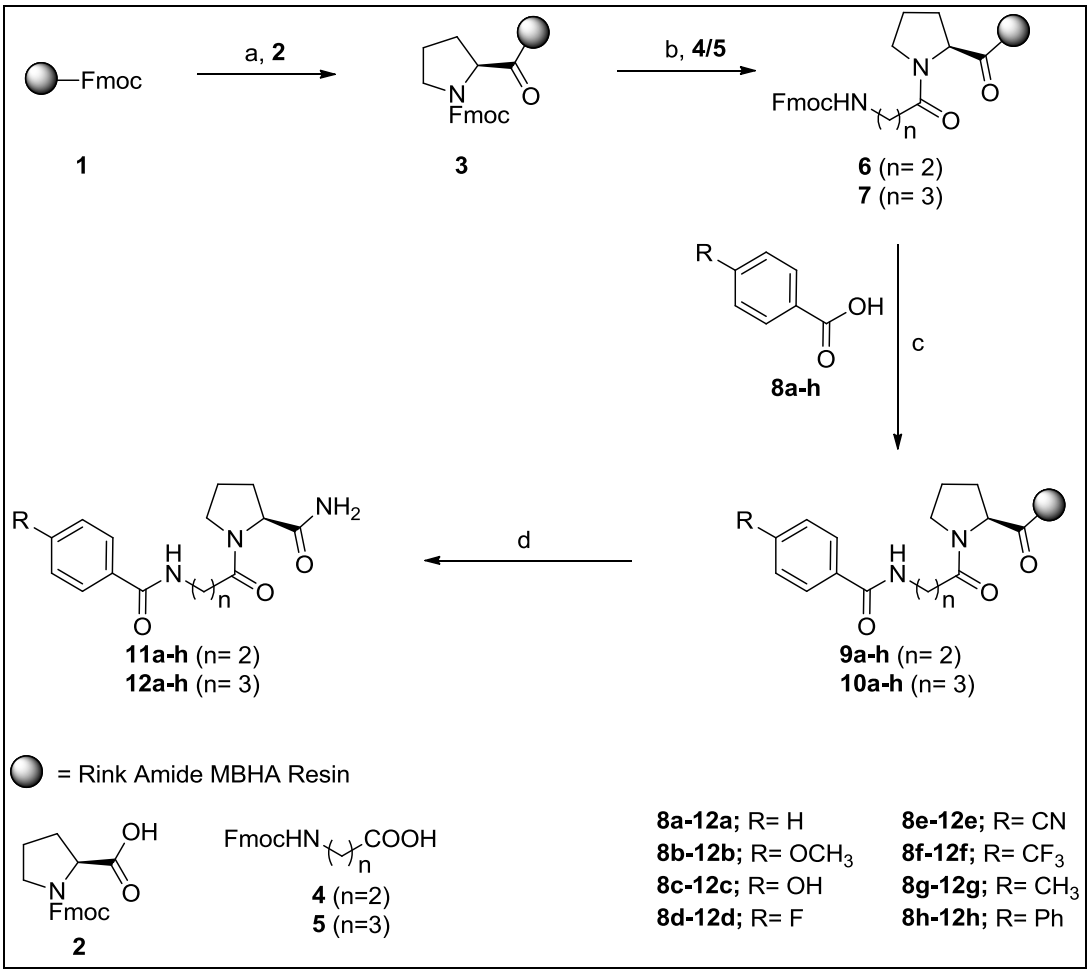

Reagents and conditions: (a) i. 20% Piperidine in DMF ii. Fmoc-Pro-OH (**2**), HOBt, DIC, DMF, N_2 (b) i. 20% Piperidine in DMF ii. Fmoc-NH-$(CH_2)_n$-COOH (**4**/**5**), HOBt, DIC, DMF, N_2 (c) i. 20% Piperidine in DMF ii. Substituted benzoic acids (**8a-h**), HOBt, DIC, DMF, N_2 (d) TFA: H_2O: Triisopropylsilane (95:2.5:2.5), 25°C, 3h.

Scheme 1. Synthetic methods for the preparation of title compounds **11a-h** and **12a-h**

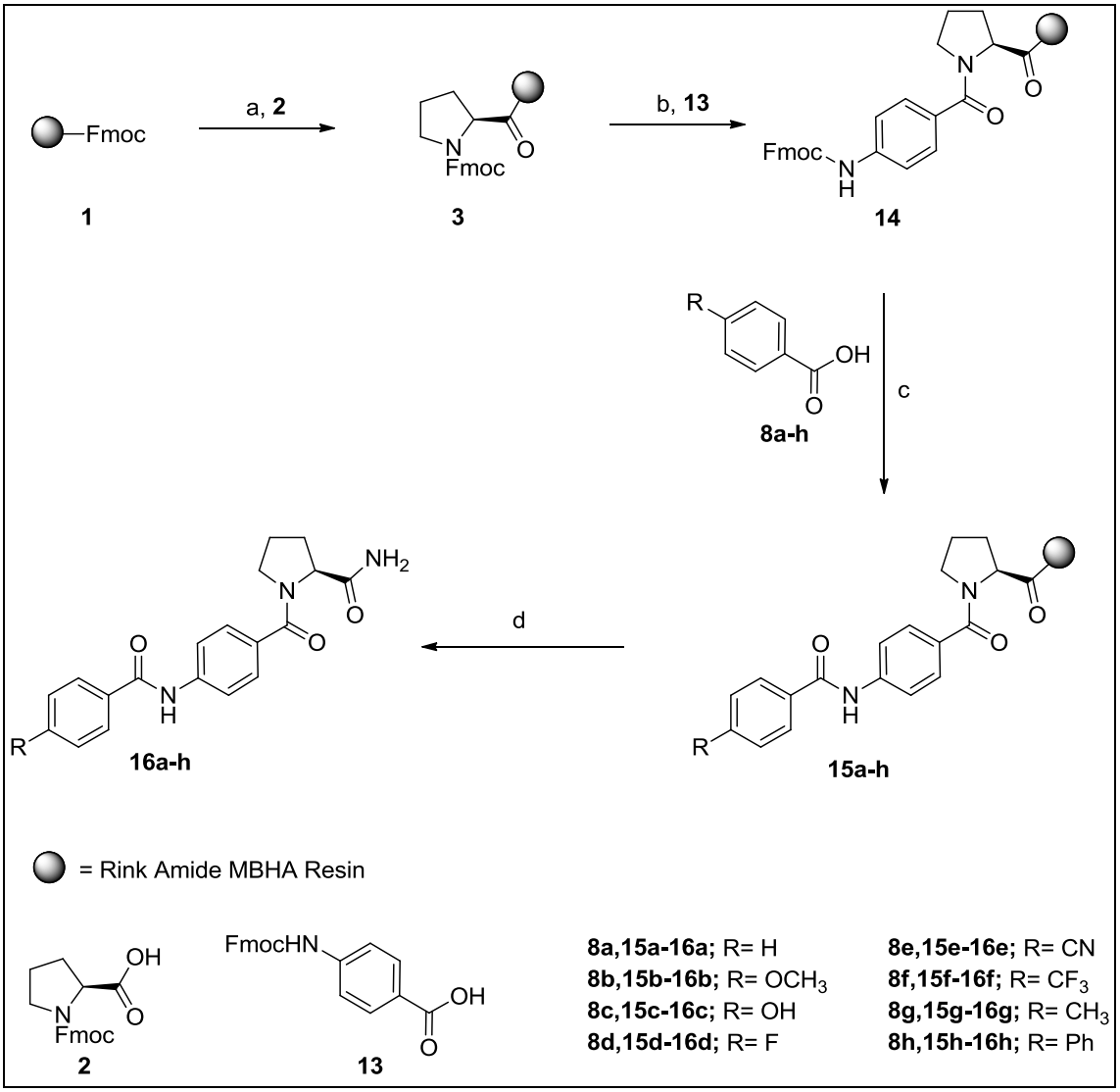

Reagents and conditions: (a) i. 20% Piperidine in DMF ii. Fmoc-Pro-OH (**2**), HOBt, DIC, DMF, N_2 (b) i. 20% Piperidine in DMF ii. Fmoc-PABA-COOH (**13**), HOBt, DIC, DMF, N_2 (c) i. 20% Piperidine in DMF ii. Substituted benzoic acids (**8a-h**), HOBt, DIC, DMF, N_2 (d) TFA: H_2O: Triisopropylsilane (95:2.5:2.5), 25°C, 3h.

Scheme 2. Synthetic methods for the preparation of title compounds **16a-h**.

For the preparation of title compounds **11a-h**, **12a-h, 16a-h, 17a-d** and **18a-b** (**Scheme 1**-**3**), we need to first synthesize Fmoc derivative of the commercially available unnatural amino acids proline **19**, β-alanine **20**, γ-amino butanoic acid **21** and *p*-amino benzoic acid **22**, synthesis of which is outline in **scheme 4**.

Substituted benzoic acids **8a-h** used for the synthesis of peptidomimetics **11a-h**, **12a-h, 16a-h, 17a-d** and **18a-b** were procured from the commercial bulk supplier and used as such without doing any modification or purification.

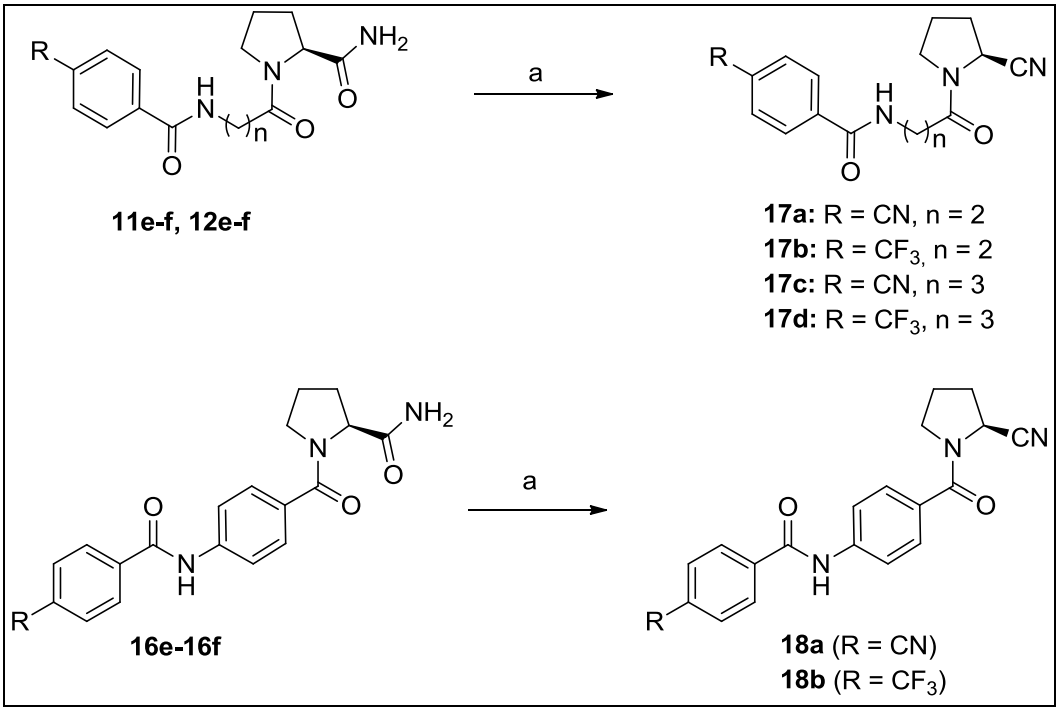

Reagents and conditions: (a) TFAA, CH_2Cl_2, 25°C, 6h.

Scheme 3. Synthetic methods for the preparation of title compounds **17a-d** and **18a-b**.

Synthesis of Fmoc deravitives of unnatural amino acids (2,4,5 and13)

In general synthesis of N-Fmoc protected amino acid is a major challenge due to racimization possibility as well as due to their zwitter ionic nature isolation problem arise. Several methods are reported in the literature for the Fmoc protection of amino acids, among which few most efficient high yielding methods are mention here. Douglass Taber et al reported convenient synthetic route to an enantiomerically pure Fmoc α-amino acid **[238]**. Manoj Gawande et al reported Fmoc protection without using any base (to avoid any racemization) at higher temperature to give desired compounds with high yield 80-95% and enantiomeric purity **[239]**. Carpino et al Fmoc-O-Su and Na_2CO_3 in a 1:1 H_2O:dioxane mixture where as more efficient method then this used by Jeffrey M. Dener utilised Fmoc-O-Su and $KHCO_3$ in a 1:1 H_2O:acetonitrile mixture **[240-241]**. Here we used different literature methods depending upon the nature of amino acids as outlined in **scheme 4** by optimizing reaction condition.

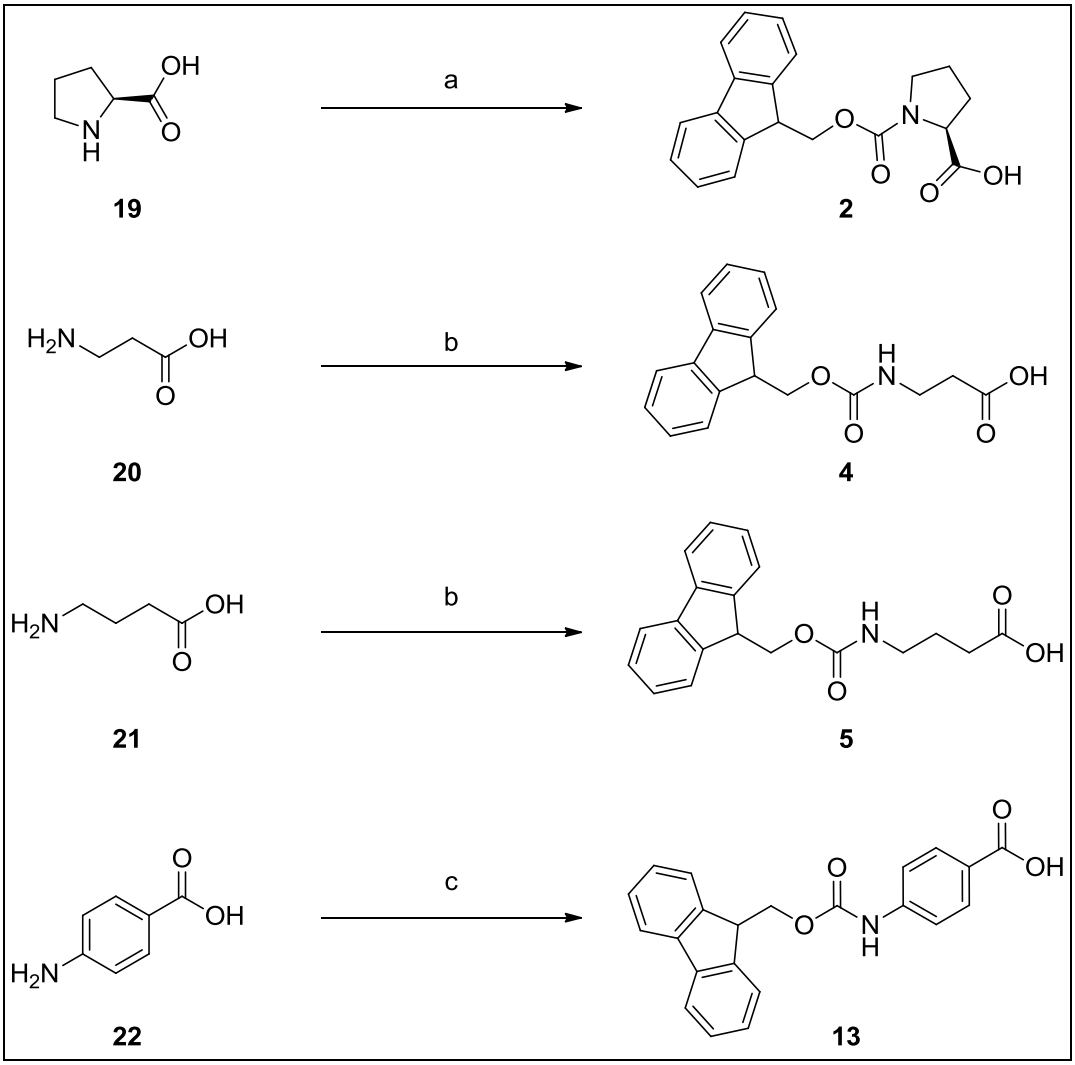

Reagents and conditions: (a) N-hydroxy succinamide, Fmoc-Cl, Na_2CO_3, Water:Acetone, 0°C-25°C, 15h (b) Fmoc-Cl, Na_2CO_3, Water:1,4 Dioxane, 25°C, 15h. (c) Fmoc-OSu, NEt_3, Water:Acetonitrile, 25°C, 3h.

Scheme 4. Different conditions for the synthesis of Fmoc protected amino acids.

However, method developed by Carpino et al is used extensively as a generlised method for the synthesis of Fmoc protected aminoacids **[240]**.

3.1.2. *In vitro* DPP-IV inhibitory activity, selectivity and structure activity relationship (SAR)

All the novel peptidomimetics compounds prepared above as two different series, pyrrolidincarboxamide containing (**11a-h**, **12a-h** and **16a-h)**, and cyanopyrrolidine containg (**17a-d** and **18a-b**) peptidomimetics were subjected for the *in vitro* DPP-IV

inhibitory activity in order to establish the structure–activity relationship (SAR) using fluorescence-based assay (details experimental protocol is given in **experimental section 5.2.1**) **[242]**. As depicted in **Table 7-8**, depending upon the nature of substitution, all the compounds showed different degree of DPP-IV inhibition (IC_{50}).

Table 7: *In vitro* DPP-IV inhibitory activity of peptidomimetics **11a-h**, **12a**-**h** and **16a**-**h**∗

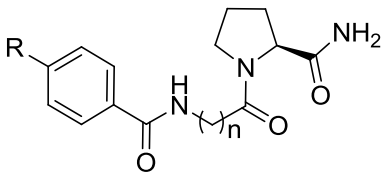

11a-h (n= 2) ; 12a-h (n= 3)

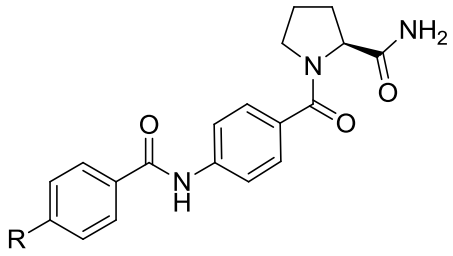

16a-h

S. No	R	DPP-IV inhibition**	S. No	R	DPP-IV inhibition**
11a	*-H*	320 ± 29	**12e**	*-CN*	26 ± 3.1
11b	*-OCH_3*	890 ± 21	**12f**	*-CF_3*	19 ± 2.3
11c	*-OH*	863 ± 18	**12g**	*-CH_3*	694 ± 14
11d	*-F*	93 ± 9.3	**12h**	*-Ph*	104 ± 16
11e	*-CN*	31 ± 2.5	**16a**	*-H*	311 ± 24
11f	*-CF_3*	28 ± 1.7	**16b**	*-OCH_3*	879 ± 22
11g	*-CH_3*	715 ± 27	**16c**	*-OH*	863 ± 13
11h	*-Ph*	107 ± 19	**16d**	*-F*	100 ± 8.5
12a	*-H*	298 ± 19	**16e**	*-CN*	34 ± 7.6
12b	*-OCH_3*	869 ± 43	**16f**	*-CF_3*	31 ± 8.3
12c	*-OH*	843 ± 26	**16g**	*-CH_3*	723 ± 21
12d	*-F*	74 ± 11	**16h**	*-Ph*	116 ± 13

∗DPP-IV inhibitory activity determined by fluorescence-based assay; fluorescence measured using Spectra Max fluorometer (Molecular Devices, CA) by exciting at 380 nm and emission at 460 nm. IC_{50} determined using Graph Pad prism software

∗∗ DPP-IV inhibitory activity represented as IC_{50} (nM), expressed as the mean ±SD (n = 3)

As described earlier in designing strategy section of DPP-IV inhibitors, novel peptidomimetics of the first series were prepared by linking basic pharmacophore, a pyrrrolidine ring system (proline) with substituted benzoic acids, using suitable spacers (i.e. set-1: β-Ala (**11a-h**); set-2: GABA (**12a-h**) and set-3: PABA (**16a-h**)). In the second series (pyrrolidinecarbonitriles), six compounds (**17a-d** and **18a,b**) were prepared by replacing pyrrolidinecarboxamides with pyrrolidinecarbonitriles.

Within the first series (**11a-h**, **12a**-**h**, **16a**-**h**), the set-1 (**11a-h**) containing *β*-alanine spacer attached to *para*-substituted benzamides, showed diverse DPP-IV inhibitory activity depending on the nature of substituents at the *para*-position. Compounds with electron donating groups (**11b**: -OMe and **11c**: -OH) showed weak inhibitory activity relative to that of un-substituted (**11a**: -H), whereas compounds with electron withdrawing groups (**11d**; **11e** and **11f**) showed good DPP-IV inhibitory activity. Among the **11d**, **11e** and **11f** tested, **11e** and **11f** showed improved DPP-IV inhibitory activity, which could be due to increase in the electronegativity at *para*-position of benzamide. Aliphatic substitution at *para* position (**11g**; $-CH_3$) showed weak inhibitory activity, while aromatic substitution at *para* position (**11h**; -Ph) showed moderate DPP-IV inhibitory activity. The second and third set of compounds (**12a**-**h**, **16a**-**h**) comprising GABA and PABA spacers attached to *para*-substituted benzamides, showed similar trend in DPP-IV inhibitory activity as observed with first set of compounds, with respect to nature of *para*-substituents.

The first series was specifically designed to understand the role of spacer and effect of *para*-substituents on benzamide. The SAR study of first series reveals that the DPP-IV inhibitory activity of test compounds drastically varies with *para*-substituents, whereas alteration in spacers (aliphatic with two/ three carbon chain-length versus aromatic) do not exhibit significant change. In general, neutral effect of spacers on inhibitory activity might be due to the flexibility in S2 pocket and stapled orientation of Glu-dyad. Substituents on *para*-position of benzamide altered inhibitory activity to greater extent because in S3 pocket, para-substituents play crucial role for its interaction with Ser209, Arg358 and Phe357.

From first series, altogether in three different sets, **11e**, **11f**, **12e**, **12f**, **16e** and **16f** (*para*-nitrile/ trifluoromethyl benzamide) were identified as primary lead compounds. Further to study effect of nitrile group on pyrrolidine ring system, a second series (**17a**-**d** and **18a**-**b**) was prepared by replacing pyrrolidinecarboxamides of first series lead compounds with pyrrolidinecarbonitriles.

As depicted in **Table 8**, all the six compounds (**17a**-**d** and **18a**-**b**) from second series showed potent inhibitory activity and was found to be comparable with standard compounds (NVP-DPP728 and Vildagliptin) **[32, 233]**. Compared to first series (pyrrolidinecarboxamides), significant improvement in the inhibitory activity was observed with second series (pyrrolidinecarbonitriles) of compounds (**17a**-**d** and **18a**-**b**), which could be due to the favorable interactions of pyrrolidinecarbonitriles with the key

residues of S1 pocket. Among six compounds tested (second series), **17c** and **17d** were found to be equipotent as Vildagliptin.

Table 8: *In vitro* DPP-IV inhibitory activity and selectivity of peptidomimetics **17a-d** & **18a-b**∗

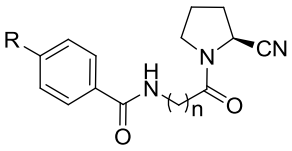

17a-b (n= 2); 17c-d (n= 3)

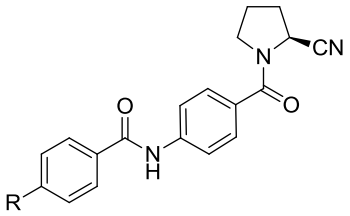

18a-b

S. No	R	DPP-IV**	DPP2$	DPP8$	DPP9$
17a	-CN	10.3 ± 1.9	---	---	---
17b	$-CF_3$	13.2 ± 2.3	---	---	---
17c	-CN	2.3 ± 0.9	>25,000	>15,000	>15,000
17d	$-CF_3$	3.8 ± 0.5	>25,000	>15,000	>15,000
18a	-CN	11.6 ± 1.6	---	---	---
18b	$-CF_3$	14.3 ± 2.5	---	---	---
NVP-DPP728#		7.2 ± 1.3	>25,000	>15,000	>15,000
Vildagliptin#		3.2 ± 0.5	---	---	---

*DPP-IV inhibitory activity determined by fluorescence-based assay.
** DPP-IV inhibitory activity represented as IC_{50} (nM), expressed as the mean ±SD (n = 3).
$ DPP2, DPP8 and DPP9 inhibitory activity represented as fold-selectivity wrt DPP-IV inhibitory activity.
# Reported literature values for NVP-DPP728 and Vildagliptin are 7±1.7 and 2.7±0.1 respectively.

The *in vitro* selectivity over serine protease, especially DPP-2, DPP-8 and DPP-9 was evaluated for most potent compounds (**17c** and **17d**) and the fold-selectivity values are listed in **Table 8** (details experimental protocol is given in **experimental section 5.2.1**). Compounds **17c** and **17d** showed >25000-fold selectivity over DPP-2 and >15000-fold selectivity over DPP-8 and DPP-9, which was found to be comparable with reference standard compounds (NVP-DDP728). Among all the compounds tested, **17c** and **17d** were found most potent and selective, hence subjected for pharmacodynamic (PD) as well as pharmacokinetic (PK) profiling studies in animal models.

3.1.3. *In vivo* antidiabetic activity of selected compounds (**17c** and **17d**)

The *in vivo* antidiabetic activity of **17c**, **17d** and NVP-DPP728 (@ 20 mg/kg, p.o.) was evaluated in male C57BL/6J mice, using IPGTT (intraperitoneal glucose tolerance test) protocol and changes in serum glucose levels (AUC glucose up to 240 min; mg/dL) are shown in **Figure 25** (details experimental protocol is given in **experimental section 5.2.3**) **[243-244]**. Compound **17c** showed good oral antidiabetic activity (% Decrease in AUC glucose 54.9 ± 3.86), whereas **17d** and NVP-DPP728 (positive control) showed moderate activity upon oral administration (% Decrease in AUC glucose 17.4 ± 5.35 and 21.5 ± 6.1 respectively). In C57 mice (IPGTT protocol), it was interesting to observe that **17c** showed suppression in the blood glucose at all the time points (30, 60, 120 and 240 min) compared to vehicle control, while **17d** and NVP-DPP728 showed reduction in blood glucose at 30 and 60 minutes.

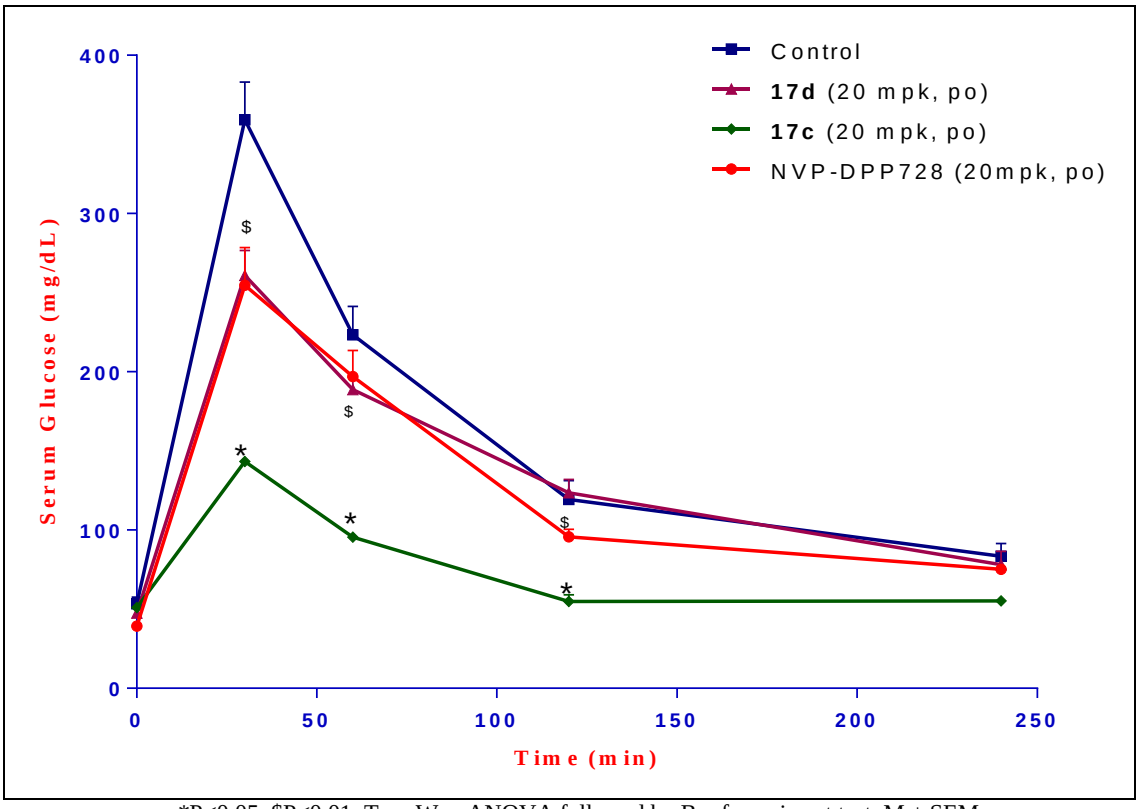

*P<0.05, $P<0.01, Two-Way ANOVA followed by Bonferroni post test, M ± SEM

Figure 25. *In vivo* antidiabetic activity of **17c**, **17d** and NVP-DPP728 in C57 mice (OGTT)

Further to understand the duration of action and effect of test compounds on post-prandial glucose excursion, single dose (@ 20 mg/kg, p.o.) antidiabetic activity of

17c and NVP-DPP728 was evaluated in fed-db/db mice (hyperglycemic animals) for 24h (**Figure 26**). Under fed condition, compared to vehicle control, NVP-DPP728 and **17c** showed good antidiabetic activity (% Decrease in AUC glucose 31.4±8.7 and 33.5 ± 7.4, respectively) up to 2h. However, **17c** showed sustained suppression in serum glucose levels for > 8h (% Decrease in AUC glucose, 14.9 ± 6.3 for NVP-DPP728 and 30.8±6.2 for **17c**, after 8h).

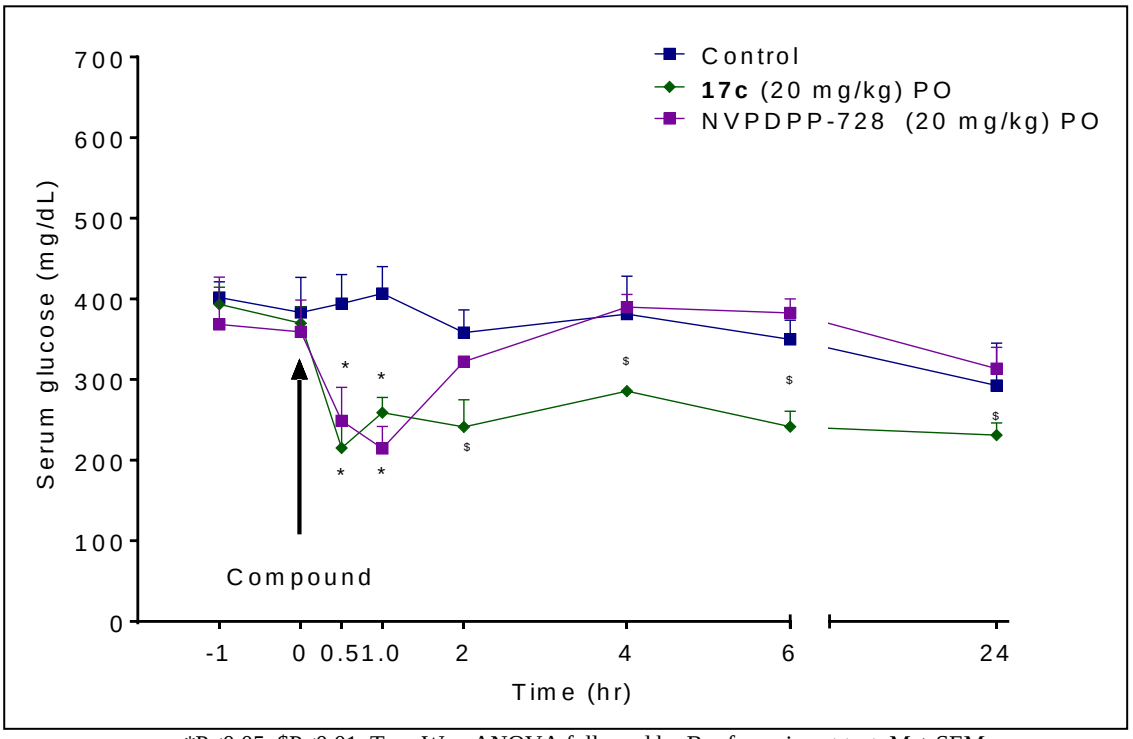

*P<0.05, $P<0.01, Two-Way ANOVA followed by Bonferroni post test, M ± SEM

Figure 26. *In vivo* antidiabetic activity of **17c** and NVP-DPP728 in db/db mice

3.1.4. Pharmacokinetic (PK) studies of selected compounds (**17c** and **17d**)

A comparative single dose (20 mg/kg i.v. or p.o.) pharmacokinetic (PK) profile of **17c, 17d** and NVP-DPP728 was evaluated in male C57BL/6J mice (n=6) and the various PK parameters such as Tmax, $t_{1/2}$, Cmax, AUC and %F were recorded as shown in **Table 9** (details experimental protocol is given in **experimental Section 5.3**). In PK study, all the test compounds showed rapid t_{max}, good C_{max} and oral bioavailability (%F ~ 63 to 72 %). Compound **17c** showed higher area under the curve (AUC: > 2-fold compared to **17d** and NVP-DPP728) and extended half-life ($t_{1/2}$: >7h compared to **17d** and NVP-DPP728). Thus improved pharmacokinetic profile of compound **17c** justifies its potent and extended pharmacodynamic effects (antidiabetic activity) in C57 and db/db mice, when administered orally.

Table 9: Pharmacokinetic study parameters[a] of **17c, 17d** and **NVP-DPP728**

Compd	Tmax (h)	Cmax (mg/ml)	$T_{1/2}$ (h)	AUC (0-α) h mg/ml	%F*
17c	0.29 ± 0.11	7.1 ± 0.83	7.99 ± 0.33	14.3 ± 1.13	72.5%
17d	0.28 ± 0.10	5.9 ± 0.88	0.99 ± 0.14	6.89 ± 1.21	63.1%
NVP-DPP728	0.32 ± 0.08	6.2 ± 0.91	0.88 ± 0.11	6.49 ± 1.11	65%

[a]In male C57BL/6J mice (n=6), compounds were administered orally (p.o) at 20 mg/kg dose and plasma concentration was analyzed by LC-MS, values indicate Mean ± SD.
* Oral bioavailability (%F) was calculated wrt to iv AUC (**17c**: 11.02 ± 0.11; **17d**: 10.92 ± 0.12 & NVP-DPP728: 9.98 ± 0.09 h µg/ml) administered at 20 mg/kg dose, iv.

3.1.5. Molecular docking study of peptidomimetic 17c

The molecular docking analysis of **17c** and NVP-DPP728 was carried out using extra precision (XP) Glide docking method, to understand its critical interactions with all the three binding sites (S1, S2 and S3) of DPP-IV enzyme (**Figure 27**) **[245-246]**. The crystal structure of the DPP-IV enzyme (PDB ID: 2I03) was obtained from the protein data bank and the protein structure was prepared using protein preparation wizard module of Schrödinger. After protein structure was prepared, the bound ligand of receptor was defined as grid binding box. For docking study, the ligands were minimized by applying an OPLS-AA forcefield, using ligprep module of Schrödinger (details experimental protocol is given in **experimental section 5.4**).

The overlay of binding poses of **17c** (Turquoise) and NVP-DPP728 (Rose) in the DPP-IV active site is shown in **Figure 27** (the molecular surface is shown in Green, the inhibitor in stick representation). The docking study results illustrate that both the compounds interact closely with key residues of S1 (cyanopyrrolidine-CN form covalent bond with OH-group of side-chain of Ser630); S2 (benzamide-NH form H-bonding with C=O groups of side-chains of Glu205 and Glu206 dyad) and S3 (aromatic–CN forms H-bonding with the NH of guanidine side-chain of Arg358) pockets (**Figure 28**).

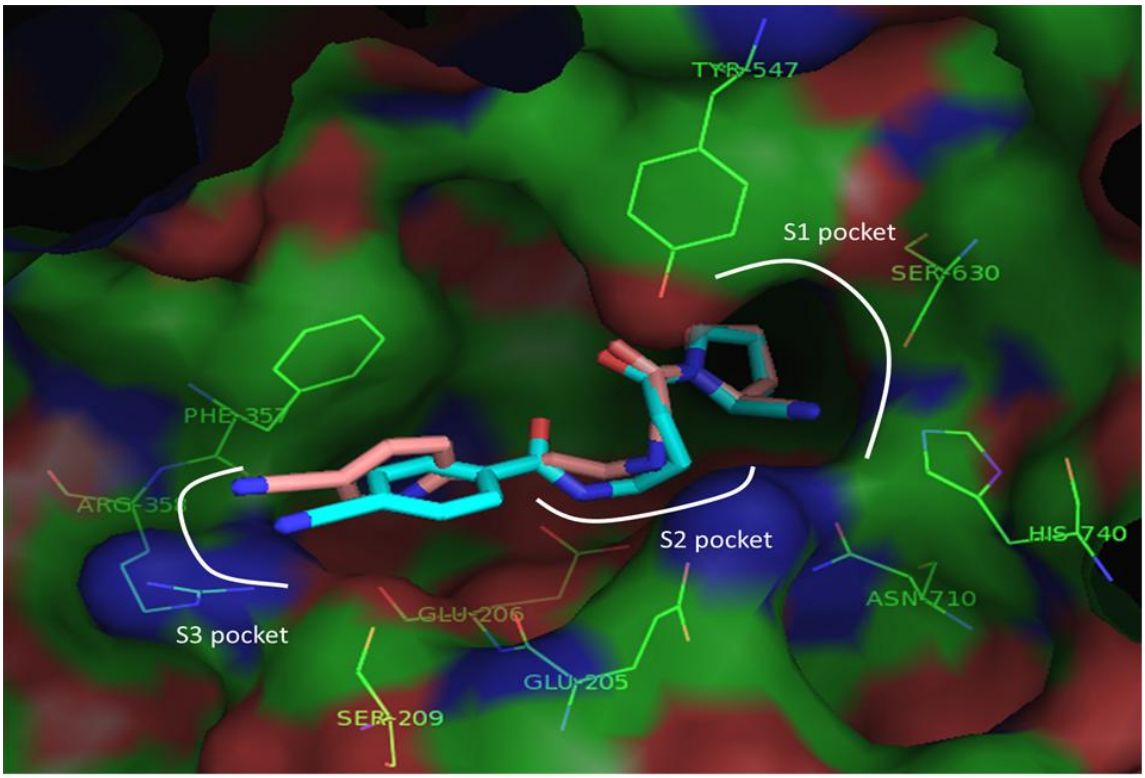

Binding pose of compound **17c** (Turquoise) and **NVP-DPP728** (Rose) in the DPP-IV active site is indicated (Surface view: Green),
wherein both compounds interact closely with key residues of site S1, S2 and S3.

Figure 27: Key interactions of compound **17c** and NVP-DPP728 (Overlay pose) with active sites of DPP-IV enzyme

Incorporation of GABA linkage (spacer) in **17c** allows it to adopt new confirmation, which favors covalent interaction of cyanopyrrolidine ring with Ser630 (S1 pocket), strong H-bonding of back-bone amide with Glu dyad (S2 pocket) and *para*-nitrile benzamide with Arg358, including aromatic π- π stacking with Phe357 in S3 pocket. As observed with NVP-DPP728, **17c** docks very well into all the three sites (S1, S2 and S3) of DPP-IV crystal structure and these favorable interactions of **17c** with all the three sites of DPP-IV enzyme support its potent *in vitro* DPP-IV inhibitory activity and excellent selectivity over other protease.

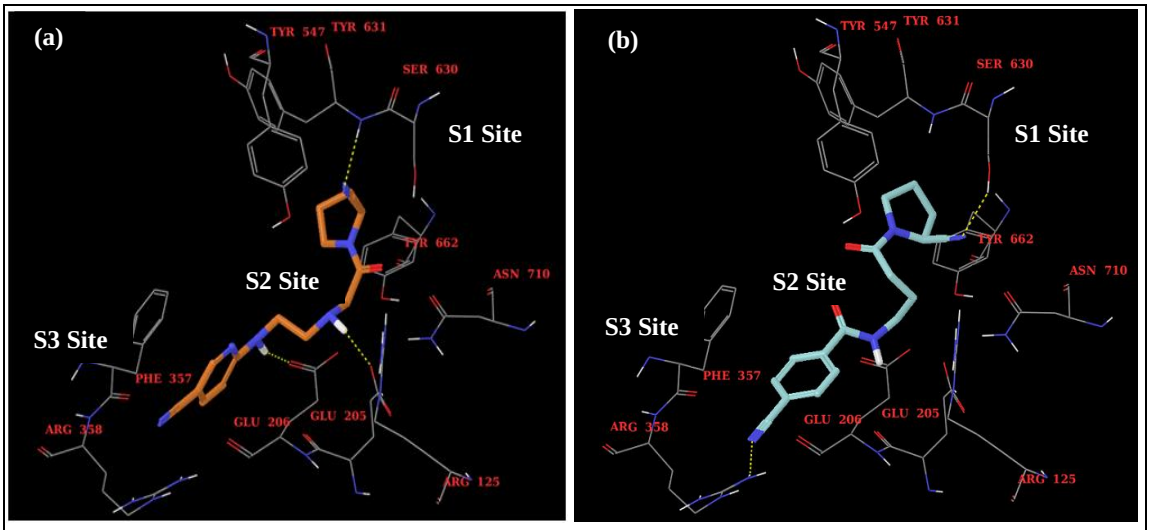

Binding pose of **NVP-DPP728** (orange) and **17c** (Turquoise) in the DPP-IV active site is indicated, wherein both compounds interact closely with key residues of site S1, S2 and S3. In site S1, cyanopyrrolidine-CN form covalent bond with OH of side chain of Ser630; S2 site, benzamide-NH…C=O groups of side chains of Glu205 & Glu206 dyad and in S3 site, Aromatic –CN…NH of guanidine side chain of Arg358.

Figure 28: Key interactions of compound **17c** and NVP-DPP728 with active sites of DPP-IV enzyme

3.1.6. Conclusion

In summary, we report here SPPS approach to discover cyanopyrrolidine containing peptidomimetic based potent DPP-IV inhibitors. Total thirty peptidomimetics have been synthesized. The peptidomimetics consisting of *para*-nitrile/-trifluoromethyl benzamide attached to cyanopyrrolidine ring with GABA spacer showed excellent *in vitro* potency and selectivity over other serine protease, due to its favorable orientation across all the three binding sites. The lead compound **17c** showed sustained suppression of pre- and post-prandial blood glucose levels (*in vivo*), which correlates with its extended half-life.

3.2. Peptidomimetic based DPP-IV inhibitors, devoid of CYP liabilities (Second series)

3.2.1. Chemistry

As discussed earlier in designing section **2.1.2.** this series was designed specially to overcome CYP activity, as because of it further development of the lead compound **17c** of the first series has been halted. Based upon the designing herein we intended to synthesize the compounds represented by general structures **27a-j** and **34a-**

m (**Figure 24**). Synthetic methodology was designed based on the retrosynthetic analysis and the schemes are described below. Synthetic method reported in literature were adapted for the synthesis of title compounds **27a-j** and **34a-m**. All compounds were synthesized following the procedure reported earlier in literature by choosing the appropriate starting materials and optimizing reaction conditions.

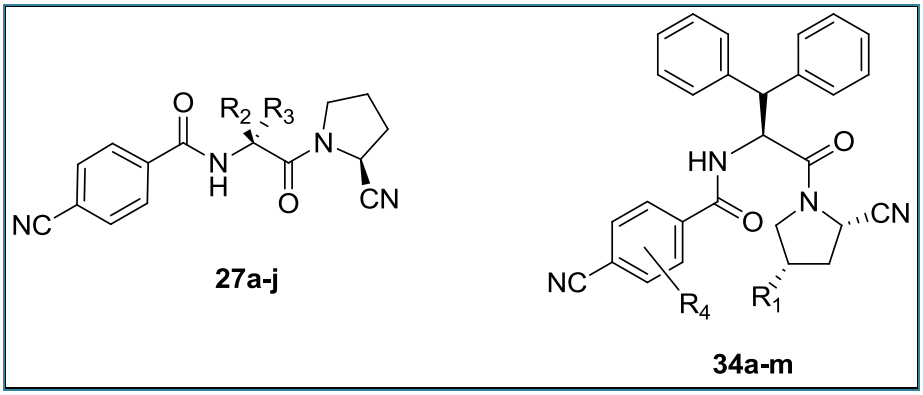

Figure 29. Peptidomimetics based DPP-IV inhibitors.

Synthesis of designed peptidomimetics **27a-j** and **34a-m** was carried out using Fmoc-based Solid Phase Peptide Synthesis (SPPS) approach illustrated in **Schemes 5-6 [237]**, starting from commercially available Rink-amide MBHA resin **1**, Deprotection of **1** with 20% piperidine in DMF and 1,3-diisopropylcarbodiimide (DIC) coupling with Fmoc-protected amino acid Proline **2** or 4-Fluoro proline **28** gave the resin-bouned Fmoc-protected amino acid **3** and **29**. Which upon deprotection with piperidine (20% DMF) and 1,3-diisopropycarbodiimide (DIC) coupling with Fmoc-protected amino acids **23a-j** provided the resin-bound Fmoc-protected dipeptides **24a-j** and **30a-b**. Deprotection of **24a-j** and **30a-b** with piperidine (20% DMF) and DIC coupling with substituted benzoic acids **8e** or **31a-k** gave resin-bound tripeptides **25a-j** and **32a-m**, which upon Trifluroacetic acid (TFA) mediated cleavage gives pyrrolidinecarboxamides (**26a-j** and **33a-m**). Trifluroacetic anhydride (TFAA) mediated dehydration of pyrrolidinecarboxamides **(26a-j** and **33a-m**) afforded title compounds as pyrrolidinecarbonitriles (**27a-j** and **34a-m**). All the test compounds obtained were purified by preparative HPLC (yield 70-85%; HPLC purity >97%) and characterized by various spectroscopic techniques.

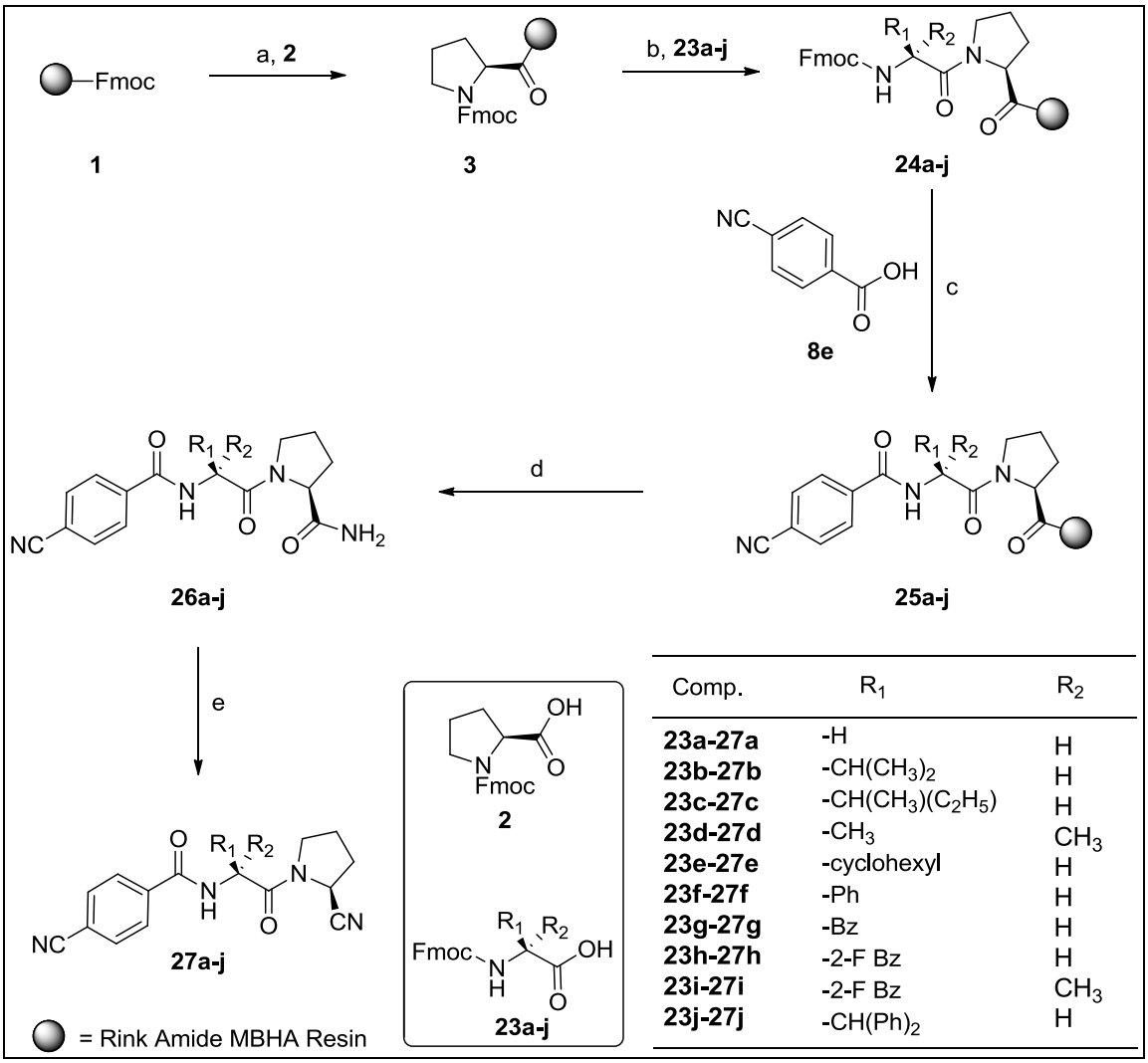

Comp.	R_1	R_2
23a-27a	-H	H
23b-27b	$-CH(CH_3)_2$	H
23c-27c	$-CH(CH_3)(C_2H_5)$	H
23d-27d	$-CH_3$	CH_3
23e-27e	-cyclohexyl	H
23f-27f	-Ph	H
23g-27g	-Bz	H
23h-27h	-2-F Bz	H
23i-27i	-2-F Bz	CH_3
23j-27j	$-CH(Ph)_2$	H

Reagents and conditions: (a) i. 20% Piperidine in DMF ii. Fmoc-Pro-OH (**2**), HOBt, DIC, DMF, N_2 (b) i. 20% Piperidine in DMF ii. Fmoc-NH-(CHR_1R_2)-COOH (**23a-j**), HOBt, DIC, DMF, N_2 (c) i. 20% Piperidine in DMF ii. *p*-cyano benzoic acid (**8e**), HOBt, DIC, DMF, N_2 (d) TFA: H_2O: Triisopropylsilane (95:2.5:2.5), 3h. (e) TFAA, CH_2Cl_2, 25°C, 6h.

Scheme 5. Synthetic methods for the preparation of peptidomimetics **27a-j**

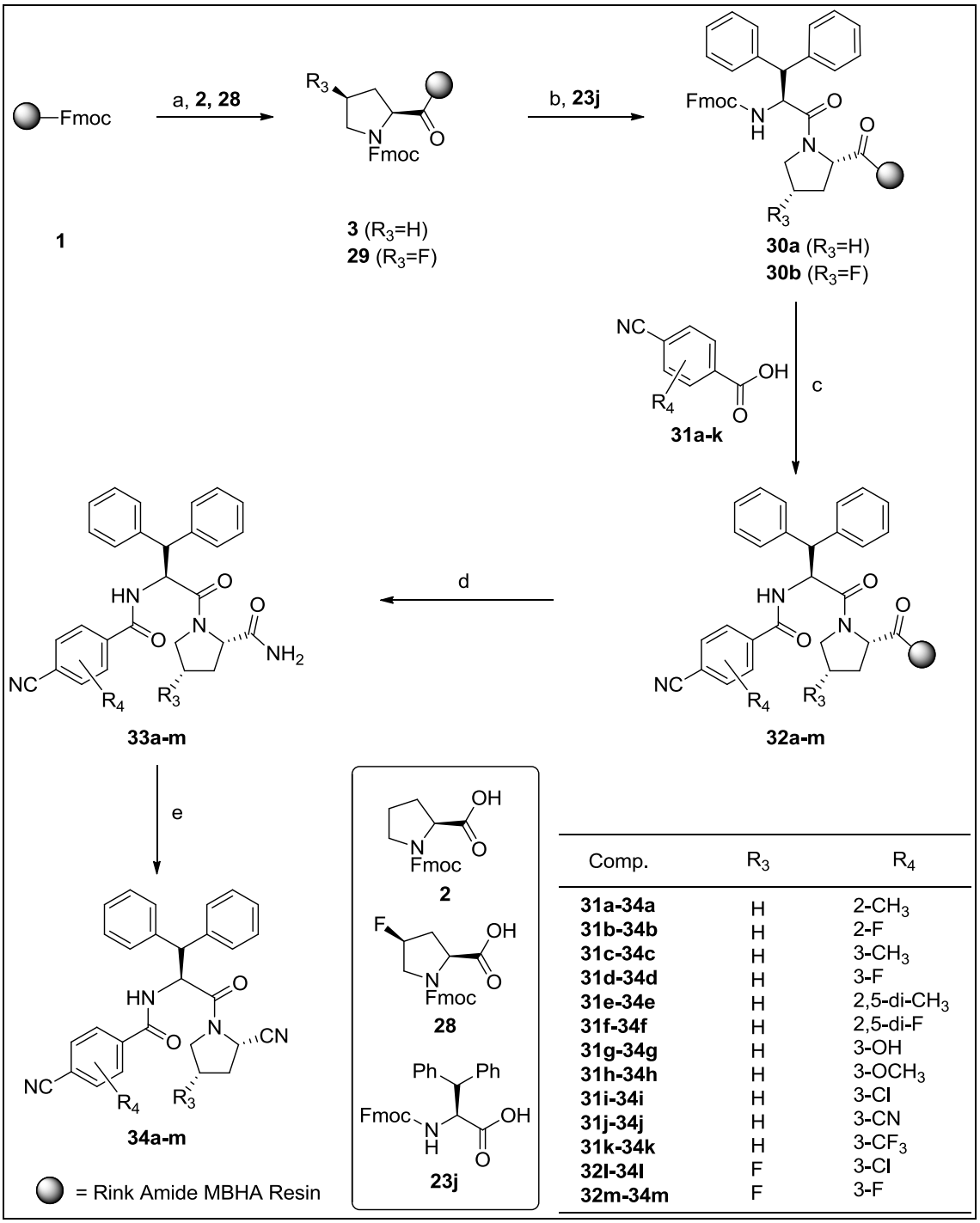

Comp.	R_3	R_4
31a-34a	H	2-CH_3
31b-34b	H	2-F
31c-34c	H	3-CH_3
31d-34d	H	3-F
31e-34e	H	2,5-di-CH_3
31f-34f	H	2,5-di-F
31g-34g	H	3-OH
31h-34h	H	3-OCH_3
31i-34i	H	3-Cl
31j-34j	H	3-CN
31k-34k	H	3-CF_3
32l-34l	F	3-Cl
32m-34m	F	3-F

Reagents and conditions: (a) i. 20% Piperidine in DMF ii. Fmoc-Pro-OH (**2**)/Fmoc-4-F-Pro-OH (**28**), HOBt, DIC, DMF, N_2 (b) i. 20% Piperidine in DMF ii. Fmoc-NH-($CHPh_2$)-COOH (**23j**), HOBt, DIC, DMF, N_2 (c) i. 20% Piperidine in DMF ii. Substituted benzoic acids (**30a-k**), HOBt, DIC, DMF, N_2 (d) TFA: H_2O: Triisopropylsilane (95:2.5:2.5), 3h. (e) TFAA, CH_2Cl_2, 25°C, 6h.

Scheme 6. Synthetic methods for the preparation of peptidomimetics **34a-m**

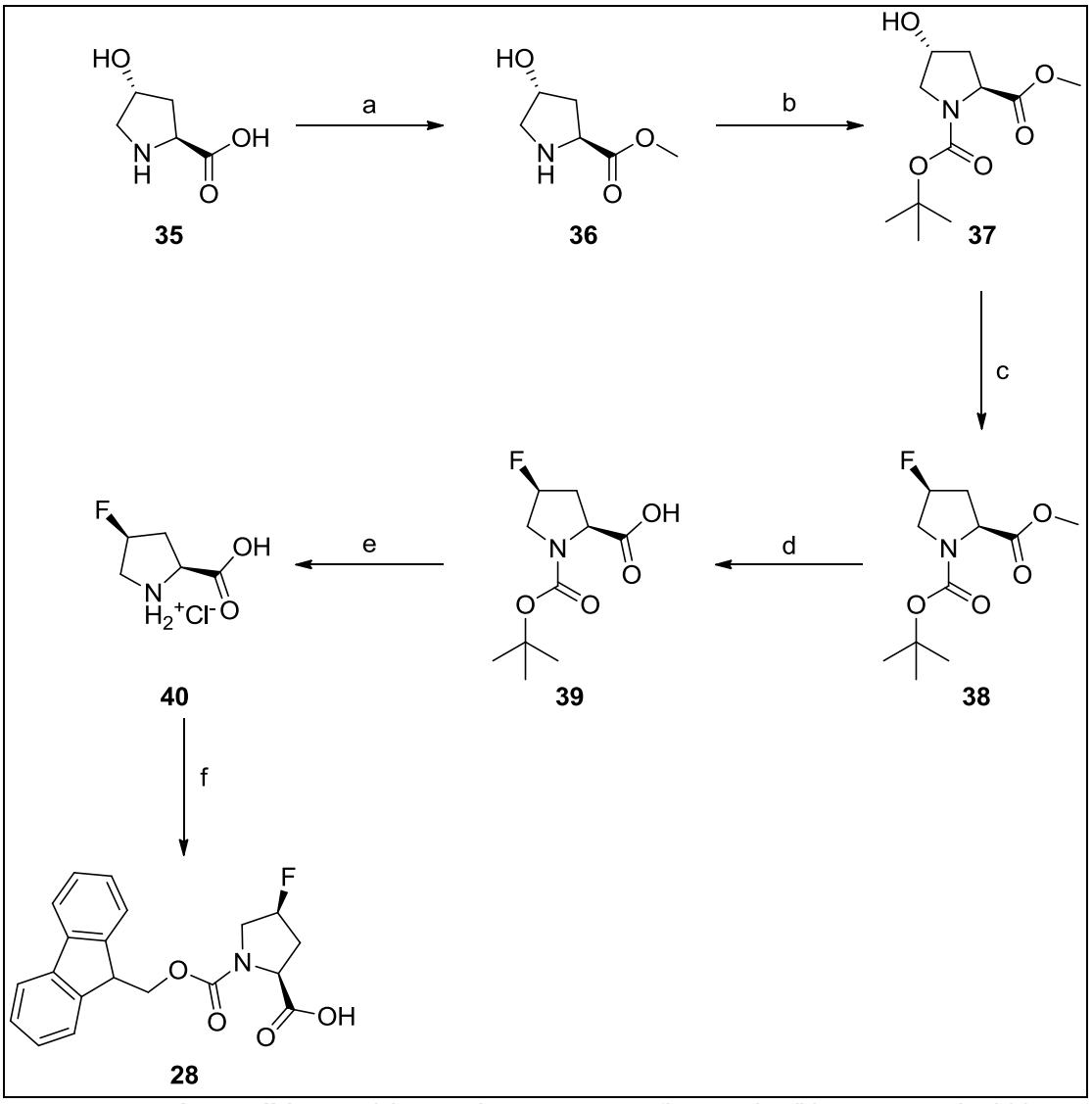

Reagents and conditions: (a) $SOCl_2$, MeOH, Reflux, 15h (b) BOC-anhydride, NEt_3, Water:Acetonitile, 0°C-25°C. 15h (c) DAST, dry DCM, -78°C-25°C, 5h (d) $NaOH_{(aq)}$, THF: MeOH (e) 4M HCl in 1,4-Dioxane, DCM, 25°C (f) N-hydroxy succinamide, Fmoc-Cl, Na_2CO_3, Water:Acetone, 0°C-25°C, 15h

Scheme 7. Synthetic methods for the preparation of unnatural amino acid **28**

However amino acids **23a-h** are commercially available so procured from commercial source and used as such. Synthesis of the unnatural aminoacids **23i-j** used to synthesize novel peptidomimetics **27a-j** and **34a-m** is illustrated in **schemes 7-9**. Christophe Dugave et al reported synthesis of 4-Fluoro prolines from commercially available trans-4-hydroxy proline methyl ester with optimum yield **[247]**. Mukund Chorghade et al reported synthesis of fluoro prolines from trans-4-hydroxy proline using tetrabutyl ammonium fluoride as a fluorine source but the yields were low **[248]**. Weiping

Zhuang et al synthesized fluoro prolines with good yields as well as chiral purity using perfluoro-1-butanesulfonyl fluoride and tetrabutylammonium triphenyldifluorosilicate (PBSF-TBAT) as a fluoride source **[249]**. Here we used method of Christophe Dugave et al for the synthesis of chiral pure Fmoc protected (2S, 4S) 4-hydroxy proline **28** by optimizing the reaction conditions (**Scheme-7**).

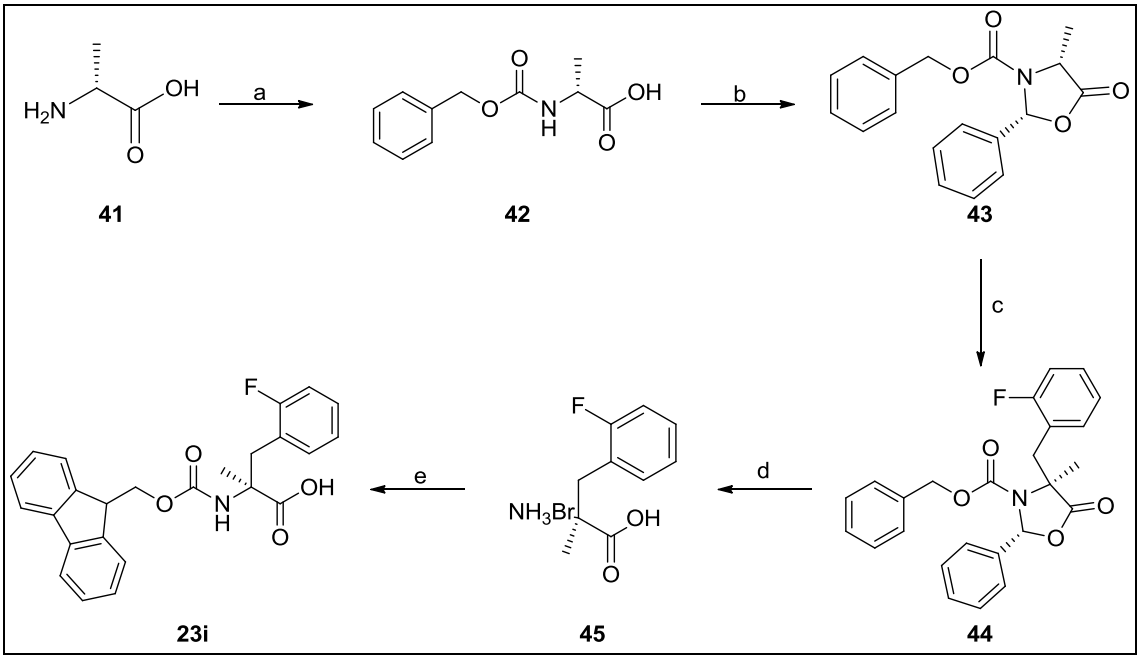

Reagents and conditions: (a) $NaOH_{(aq)}$, Cbz-Cl, Acetonitrile, 0°C-25°C, 15h (b) Benzaldehyde dimethyl acetal, $SOCl_2$, $ZnCl_2$, THF, 0°C 4h (c) 2-F Benzyl bromide, KHMDS, THF, -27°C (d) 33%HBr in CH_3COOH, CH_3COOH, 25°C, 20h (e) Fmoc-Cl, Na_2CO_3, Water:1,4-Dioxane, 0°C-25°C, 15h.

Scheme 8. Synthetic methods for the preparation of unnatural amino acid **23i**

For the synthesis of α-methyl amino acids various methods are reported in the literature **[250]**. Roy Storcken et al reported a chemoenzymatic approach to the synthesis of functionalized α-methyl α-substituted amino acids which involves amidase-mediated enzymatic resolution and cross-metathesis **[251]**. Ta-Jung Lu et al reported asymmetric synthesis of α-methyl-α-amino acids via diastereoselective alkylation of (1*S*)-(+)-3-Carene derived tricyclic iminolactone with high enantiopurity **[252]**. Martin O'Donnell et al reported enantioselective synthesis of α-methyl amino acid via phase-transfer catalysis **[253]**. Franklin Davis et al reported sulfinimine-mediated asymmetric strecker synthesis of the synthesis of α-alkyl α-amino acids **[254]**. Peng-Fei Xu et al. reported synthesis of α,α-disubstituted α-amino acids by diastereoselective alkylation of camphor-based tricyclic iminolactone **[255]**.

Here we used enetioselective and high yielding method of Suresh Kapadia et al for the synthesis of amino acid **23i** as shown in **scheme-8** by modifying the reaction conditions **[256]**.

Soledad Royo et al reported high yielding racemic synthesis and a very efficient resolution procedure for synthesis of enantiomerically pure unnatural amino acid β-phenyl phenyl alanine (β-PPA) **23j [257]**. Mukund SibI et al have reported convenient synthesis of antipode of **23j** using chiral auxiliary starting from L-serine methyl ester hydrochloride in good yield and chiral purity **[258]**. Ari Koskinen et al reported very good scalable method for the preparation of enantiomer of **23j [259]**, Here we adopted this method of Ari Koskinen et al for the synthesis of **23j** by replacing the starting material with its antipode and optimizing the reaction conditions to obtaine **23j** with desire absolute (S) configuration (**scheme-9**) **[259]**.

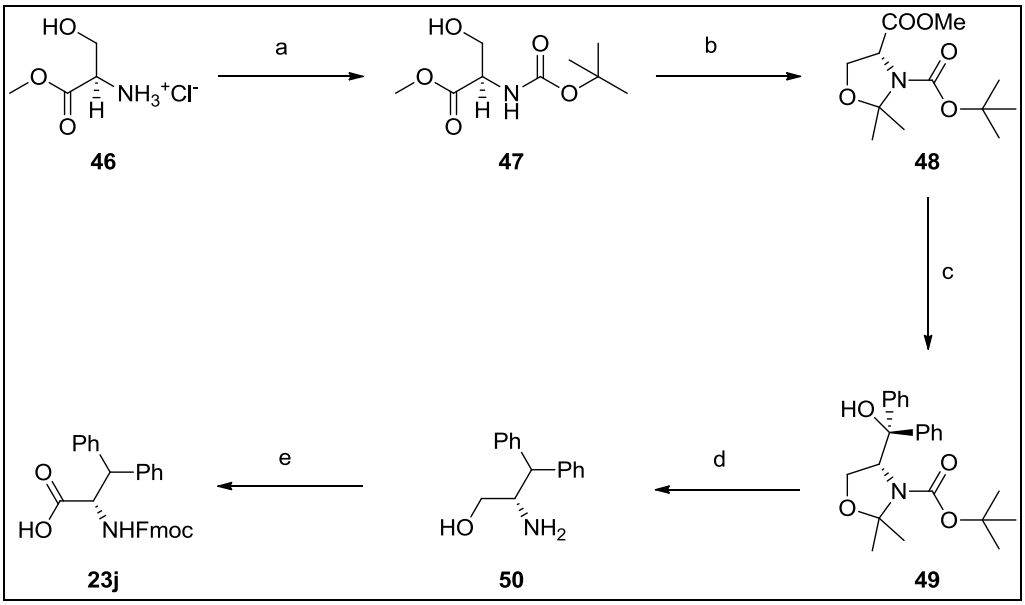

Reagents and conditions: (a) BOC-anhydride, NEt_3, Water:Acetonitrile, 0°C-25°C. 15h (b) 2,2-Dimethoxypropane, BF_3-Et_2O, Acetone, 25°C, 3h (c) PhMgBr, THF, 0°C, 5h (d) i. H_2, $Pd(OH)_2$/C, HCOOH, 60°C, 5h, ii. NaOH, MeOH:Water, reflux, 15h (e) i. Fmoc-Cl, Na_2CO_3, Water:1,4-Dioxane, 0°C-25°C, 15h, ii. CrO_3, H_2SO_4, Acetone, 0°C, 3h.

Scheme 9. Synthetic methods for the preparation of unnatural amino acid **23j**

Synthesis of **23j** was accomplished with commercially available D-Serine methyl ester hydrochloride **46**, making Garner's aldehyde type chiral auxiliary derivative **48** by adopting method reported by Andrew Campbell et al and performing necessary optimization in reaction conditions **[260]**.

However various substituted 4-cyano benzoic acids **31a-k** used for the synthesis of peptidimimetics **27a-j** and **34a-m** have been procured from the commercial suppliers and no attempt have been made for their synthesis.

3.2.2. *In vitro* DPP-IV inhibitory activity, selectivity and structure activity relationship (SAR)

The *in vitro* DPP-IV inhibitory activity was determined in order to establish the structure–activity relationship (SAR) using fluorescence-based assay (details experimental protocol is given in **experimental Section 5.2.1.**) **[242]**. As shown in **Table 10-11**, two series of peptidomimetics (**27a-j** and **34a-m**) were prepared and depending on the nature of substitutions, different degree of DPP-IV inhibitory activity was observed.

Table 10: *In vitro* DPP-IV inhibitory activity of peptidomimetics **27a-j**∗

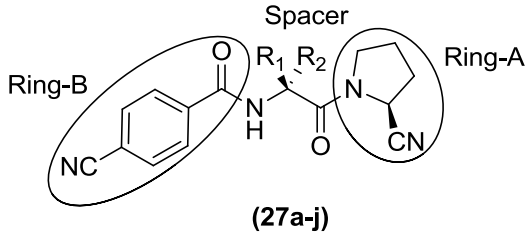

(27a-j)

S. No	R_1	R_2	Amino acids[$]	DPP-IV inhibition[**]
27a	H	-H	Gly	722 ± 3.4
27b	$-CH(CH_3)_2$	-H	Val	74 ± 2.4
27c	$-CH(CH_3)(C_2H_5)$	-H	Ile	39 ± 1.2
27d	$-CH_3$	$-CH_3$	Aib	157 ± 3.3
27e	cyclohexyl	-H	Chg	97 ± 2.7
27f	-Ph	-H	Phg	463 ± 3.8
27g	-Bz	-H	Phe	239 ± 1.9
27h	2-F Bz	-H	2-F Phe	197 ± 3.6
27i	2-F Bz	$-CH_3$	α-Me-2-F Phe	137 ± 4.9
27j	$-CH(Ph)_2$	-H	βPPA	**27 ± 1.6**
Vildagliptin	--	--	--	3.2 ± 0.5
17c	--	--	--	2.3 ± 0.9

∗DPP-IV inhibitory activity determined by fluorescence-based assay; fluorescence measured using Spectra Max fluorometer (Molecular Devices, CA) by exciting at 380 nm and emission at 460 nm. IC_{50} determined using Graph Pad prism software

∗∗ DPP-IV inhibitory activity represented as IC_{50} (nM), expressed as the mean ±SD (n = 3)

[$] **$R_1$, R_2** together represents amino acids with absolute (S) stereo configuration

In the first series, upon linking cyanopyrrolidine (ring A) with *para*-cyanobenzoic acid (ring B), using α-substituted amino acid spacers (Val; **27b**, Ile; **27c** or cyclohexyl glycine (Chg); **27e**), compounds **27b**, **27c** and **27e** showed moderate DPP-IV inhibitory activities. When amino-isobutyric acid (Aib); **27d** or α-methyl-2-fluoro phenyl alanine (α-Me-2-F Phe); **27i**, were introduced as spacer, the resulting compounds however showed weak *in vitro* activities. The compounds **27f**, **27g** and **27h** containing phenyl glycine (Phg), phenyl alanine (Phe) and 2-fluoro phenyl alanine (2-F-Phe) respectively as spacers were also found to be the least potent. However compound **27j** with β-phenyl phenyl alanine (β-PPA) showed the highest DPP-IV inhibitory activity (IC_{50}: 27 nM) within the series.

The first series was specifically designed as analogs of **27a**, to understand the role of α-substituents on 1C amino-alkyl spacer so as to get the low nM DPP-IV inhibitory activity. The SAR study of first series reveals that the DPP-IV inhibitory activity of test compounds drastically varies with the nature of α-substituents and among various substituents screened, β-PPA was found to be favorable. It appears that the DPP-IV enzyme accepts changes in limited steric bulk at S2 binding pocket, which might be due to the stapled orientation of Glu-dyad in S2 pocket.

Compound **27j** was identified as primary hit from the first series. Further to improve DPP-IV inhibitory activity of **27j**, second series (**34a-m**) was designed, specifically by carrying out suitable changes over ring-A and -B of **27j** and in second series, five sets of compounds were prepared (**Table 11**). Substitutions were carried out in set-1 (**34a** and **34b**) on 2nd position, in set-2 (**34c** and **34d**) on 3rd position and in set-3 (**34e** and **34f**) on 2nd and 5th positions of cyano-benzamide (ring-A) , either with electron withdrawing (EW) or electron donating (ED) groups. In set-4 (**34g**-**34k**), substitutions were carried out specifically on 3rd position of cyano-benzamide (ring-A). Finally, based upon the literature presidencies (favorable substitution of 4F- pyrrolidine in Denagliptin), set-5 (**34l** and **34m**) was prepared by substituting 4th position of cyano-pyrrolidine (ring-B) with fluoro group, to improve the DPP-IV inhibitory activity.

All the test compounds from the second series showed significant DPP-IV inhibitory activities. Set-1 and 2 showed improved but similar DPP-IV inhibitory activities, irrespective of electron withdrawing (EW) or electron donating (ED) nature of the substituents. Compare to Set-1 and 3, Set-2 showed very good DPP-IV inhibitory activities.

Table 11: *In vitro* DPP-IV inhibitory activity of peptidomimetics **34a-m**∗

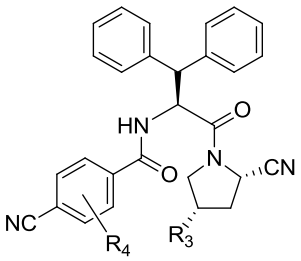

34a-m

S. No	R_3	R_4	DPP-IV inhibition**	DPP2$	DPP8$	DPP9$
34a	-H	2-CH_3	34 ± 2.9	---	---	---
34b	-H	2-F	22 ± 1.7	---	---	---
34c	-H	3-CH_3	18 ± 1.3	---	---	---
34d	-H	3-F	9.6 ± 0.6	>25,000	>15,000	>15,000
34e	-H	2,5-di-CH_3	31 ± 2.4	---	---	---
34f	-H	2,5-di-F	19 ± 0.7	---	---	---
34g	-H	3-OH	28 ± 2.7	---	---	---
34h	-H	3-OCH_3	23 ± 1.9	---	---	---
34i	-H	3-Cl	11 ± 0.8	>25,000	>15,000	>15,000
34j	-H	3-CN	17 ± 1.3	---	---	---
34k	-H	3-CF_3	14 ± 2.1	---	---	---
34l	-F	3-Cl	**4.2 ± 0.7**	>25,000	>15,000	>15,000
34m	-F	3-F	**2.7 ± 0.3**	>25,000	>15,000	>15,000
Denagliptin* **		--	19 ± 3.2	---	---	---
17c	--	--	2.3 ± 0.9	>25,000	>15,000	>15,000

∗DPP-IV inhibitory activity determined by fluorescence-based assay; fluorescence measured using Spectra Max fluorometer (Molecular Devices, CA) by exciting at 380 nm and emission at 460 nm. IC_{50} determined using Graph Pad prism software.

∗∗ DPP-IV inhibitory activity represented as IC_{50} (nM), expressed as the mean ±SD (n = 3).

$ DPP2, DPP8 and DPP9 inhibitory activity represented as fold-selectivity wrt DPP-IV inhibitory activity.

∗∗∗ Reported literature value for Denagliptin 22 nM (Ref: **[261]**)

Based on these results, further changes were made only at 3rd position of cyano-benzamide, as set-4 (**34g**-**34k**). In set-4, compounds **34j and 34k** with EW groups at *meta* position of cyano-benzamide showed higher DPP-IV inhibitory activities than compounds **34g and 34h**, with ED groups. Among all the compounds tested from second series, halo substituted compounds (**34d** and **34i**) showed excellent DPP-IV inhibitory activities (IC_{50}: 9.6 and 11 nM respectively). The 4-fluoropyrrolidine-carbonitrile derivatives (**34l** and **34m**, set-5) of **34d** and **34i** showed further improvement in DPP-IV inhibitory activities (IC_{50}: 4.2 and 2.7 nM respectively, similar to the best lead compound **17c** of our first designed series-1 discussed in section **3.1**), which could be due to the

favorable interactions of 4-fluoro pyrrolidine-carbonitrile with the key residues of S1 pocket.

The *in vitro* selectivity over serine protease, especially DPP-2, DPP-8 and DPP-9 was evaluated for most potent compounds **34d**, **34i**, **34l** and **34m** (fold-selectivity listed in **Table 11**) **[242]**. All the test compounds showed >25000-fold selectivity over DPP-2 and >15000-fold selectivity over DPP-8 and DPP-9, which was found to be comparable with reference standard compound **17c**. Among all the compounds tested, **34l** and **34m** were found to be most potent and selective.

3.2.3. *In vitro* CYP inhibition study of selected peptidomimetics.

To assess the CYP liabilities of these peptidomimetics, **34l** and **34m** were subjected for CYP3A4 and CYP2D6 inhibition studies (details experimental protocol is given in **experimental Section 5.2.2.**). Both the test compounds were found to be devoid of CYP3A4 and CYP2D6 inhibition up to 100 mM concentrations **[262]**.

3.2.4. Molecular docking study of lead peptidomimetic 34m

The molecular docking analysis of **27a**, **34m** and **Denagliptin** was carried out using extra precision (XP) Glide docking method (**Figure 30**), to understand their critical interactions with all the three binding sites (S1, S2 and S3) of DPP-IV enzyme (**Figure 31**; binding poses overlay of **27a** (Turquoise), **34m** (Brown) and **Denagliptin** (Rose)). The crystal structure of the DPP-IV enzyme (PDB ID: 2I03) was obtained from the protein data bank and the protein structure was prepared using protein preparation wizard module of Schrödinger (details experimental protocol is given in **experimental section 5.4**) **[245-246]**.

The results of docking studies illustrate that all the three compounds interact closely with the key residues of S1 pocket (as per literature presidencies, cyanopyrrolidine-CN may form covalent bond with OH-group of side-chain of Ser_{630}). In S_2 pocket, benzamide-NH of **34m** and α-amino group of Denagliptin forms H-bonding with C=O groups of side-chains of Glu205 and Glu206 dyad, while benzamide-NH of **27a** flip away from the Glu dyad. Compound **34m** interact closely in S3 pocket (aromatic–CN forms H-bonding with the NH of guanidine side-chain of Arg_{358}), while **27a** interact

weakly with the key residues of S2 and S3 pockets, which may justify its weak *in vitro* DPP-IV inhibitory activity.

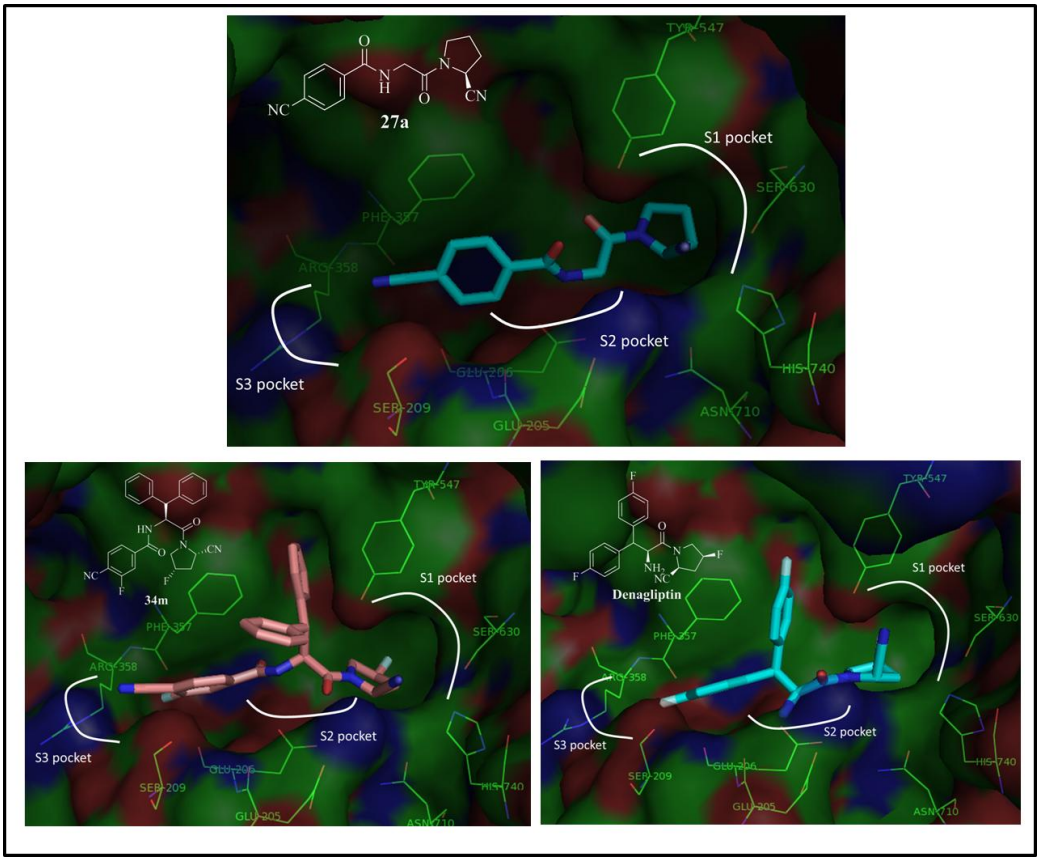

Figure 30: Key interactions of compounds **27a**, **34m** and **Denagliptin** with active sites of DPP-IV enzyme

Incorporation of β-PPA linkage (spacer) in **34m** allows it to adopt new confirmation, which may favors covalent interaction of cyanopyrrolidine ring with Ser630 (S1 pocket, covalent interaction of cyanopyrrolidine ring, as reported for cyanopyrrolidine derivatives), strong H-bonding of back-bone benzamide-NH with Glu dyad (S2 pocket) and *para*-nitrile benzamide with Arg358, including aromatic π- π stacking of benzamide with Phe357 in S3 pocket. As observed with Denagliptin, **34m** docks very well into all the three sites (S1, S2 and S3) of DPP-IV crystal structure and these favorable interactions of **34m** across all the three sites of DPP-IV enzyme support its potent *in vitro* DPP-IV inhibitory activity and excellent selectivity over other protease.

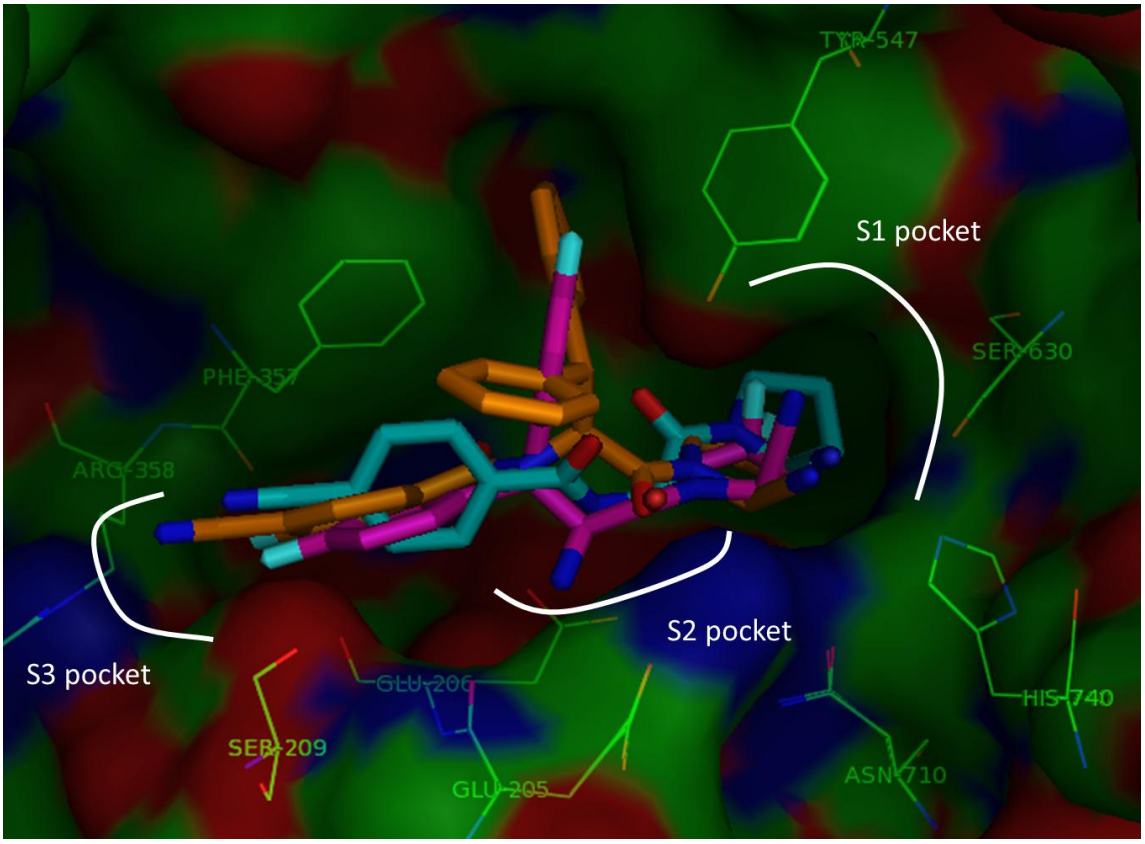

Binding pose of compound **27a** (Turquoise), **34m** (Brown) and **Denagliptin** (Rose) in the DPP-IV active site is indicated (Surface view: Green),
wherein compounds **34m** and **Denagliptin** interacts closely with key residues of site S1, S2 and S3.

Figure 31: Overlay binding pose of compounds **27a**, **34m** and **Denagliptin** with active sites of DPP-IV enzyme

3.2.5. Conclusion

In summary, we have reported discovery of peptidomimetic based cyanopyrrolidines derivatives as potent and selective inhibitors of DPP-IV and devoid of CYP liabilities. Novel peptidomimetics **34l** and **34m** showed excellent *in vitro* potency and selectivity over other serine proteases, due to their favorable orientations across all the three binding sites. Thus we successfully overcome the CYP inhibition problem arise with the lead compound **17c** of the first series by modifying it to novel peptidomimetic **34m** with no CYP inhibition up to 100 mM concentrations.

3.3. Aminomethylpiperidone based DPP-IV inhibitors (Third series)

3.3.1. Chemistry

As discussed in designing section **2.1.3** this series was specifically designed to develop potent and selective DPP-IV inhibitors with improved pharmacokinetic profile. wherein we intended to synthesize the compounds represented by general structures **68a-v**, **69a-e** and **70a-e** (**Figure 32**). Synthetic methodology was designed based on the retrosynthetic analysis and the schemes are described below. Synthetic method reported in literature were adapted for the synthesis of title compounds **68a-v**, **69a-e** and **70a-e**. All compounds were synthesized following the procedure reported earlier in literature by choosing the appropriate starting materials and optimizing reaction conditions.

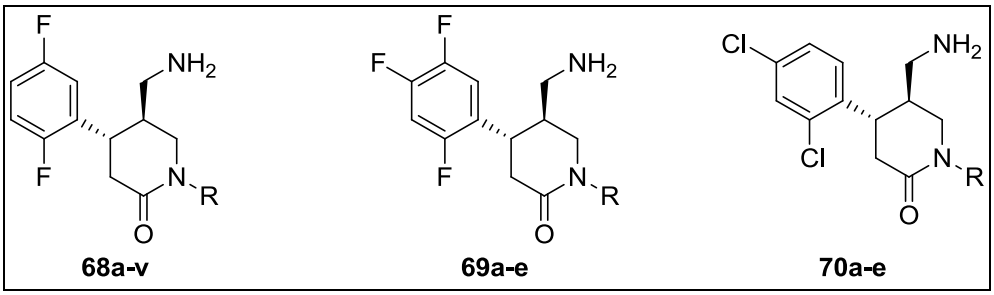

Figure 32. Aminomethyl-piperidone based DPP-IV inhibitors

As depicted in **Scheme-10**, synthesis of the aminomethyl-piperidones based DPP-IV inhibitors (**68a-v**, **69a-e** and **70a-e**) commenced with a Horner-Wadsworth-Emmons reaction of aldehydes **51a-c**, followed by Michael addition, to get diester (**53a-c**). Reduction of nitrile group of **53a-c** by hydrogenation, using Adam's catalyst, followed by cyclization and ester regeneration by trimethylsilyldiazomethane yielded piperidone-carboxylate (**56a-c**), with >85% *trans* selectivity **[263]**. *Trans* racemic mixture [(3R, 4S) and (3S, 4R)] of (**56a-c**) were isolated in pure form by removing corresponding *cis* racemic mixture [(3R, 4R) and (3S, 4S)], by column chromatography (mobile phase: 0-3% methanol in DCM, using 100-200 mesh silica gel). Amide *–NH* protection of *trans* racemic **56a-c** with *para*-methoxy benzyl (PMB) group and reduction of ester with lithium aluminium hydride ($LiAlH_4$) provided *trans* racemic alcohol (**58a-c**). Subsequently, **58a-c** were converted to a good leaving group (methanesulfonate derivatives **59a-c**), which upon treatment with potassium phthalimide via Gabriel synthesis type reaction lead to the formation of *trans* racemic phthalimido-piperidones (**60a-c**).

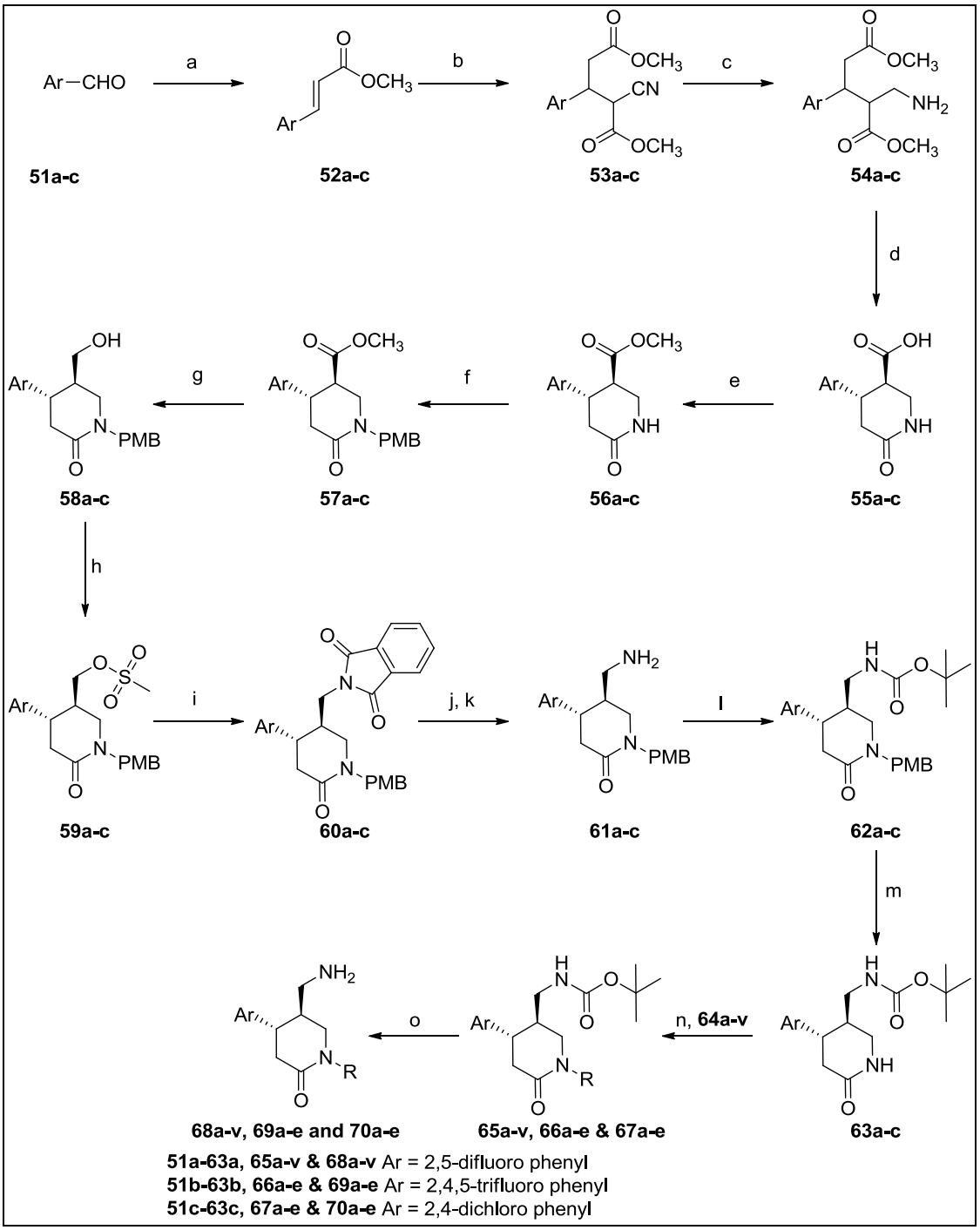

Reagents and conditions: (a) $(Et_2O)_2POCH_2COOMe$, Na_2CO_3, EtOH (b) $NCCH_2COOMe$, NaOMe, MeOH (c) H_2, PtO_2, HCl, MeOH (d) K_2CO_3, Toluene/MeOH (e) Me_3SiCHN_2, Et_2O/MeOH (f) PMB-Br, NaHMDS, THF/DMF(4:1), -78°C (g) $LiAlH_4$, THF, 0°C (h) CH_3SO_2Cl, NEt_3, DCM, 0°C (i) Pottassium phthalimide, DMF, 90°C (j) NH_2-NH_2, EtOH, 25°C (k) Chiral resolution: D-tartaric acid, MeOH. (l) Boc_2O, NEt_3, THF/H_2O(3:2), 25°C (m) CAN, CH_3CN/H_2O(3:1), 25°C (n) R-X (**64a-v**), CuI, K_2CO_3/K_3PO_4, N,N'-dimethylethylenediamine, Toluene, Reflux *or* R-X (**64a-v**), NaH, DMF, 0°C-25°C (o) Conc. HCl/EtOAc(1:3), -50°C, 2h, 0°C, 1h.

Scheme 10. Synthetic methods for the preparation of aminomethylpiperidones **68a-v**, **69a-e** and **70a-e**

Hydrazinolysis of phthalimido group of **60a**-**c** provided *trans* racemic aminopiperidones (**61a-c**). *Trans* racemic **61a-c** was subjected for chiral resolution using D-tartaric acid, to get enantiomerically pure (4S, 5S) desired piperidones (**61a**-**c)** as a tartrate salt with >97% ee. Protection of primary amine with Boc-group and subsequent oxidative removal of PMB group gave Boc-aminopiperidones (**63a-c**). Various haloheterocycles/ halo-aromatics of the interest **64a-v** (**Figure 33**) were coupled with Boc-aminopiperidones (**63a-c**) by Goldberg reaction **[264]** or by nucleophilic substitution, followed by Boc-deprotection lead to the formation of chiral pure (4S, 5S) aminomethyl-piperidones (**68a-v**, **69a-e** and **70a-e**) **[265-266]**. All the test compounds obtained were purified by preparative HPLC (yield 70–85%; HPLC purity >97% and chiral purity >97%ee) and characterized by various spectroscopic techniques (^{13}C NMR, ^{1}H NMR and ESI MS).

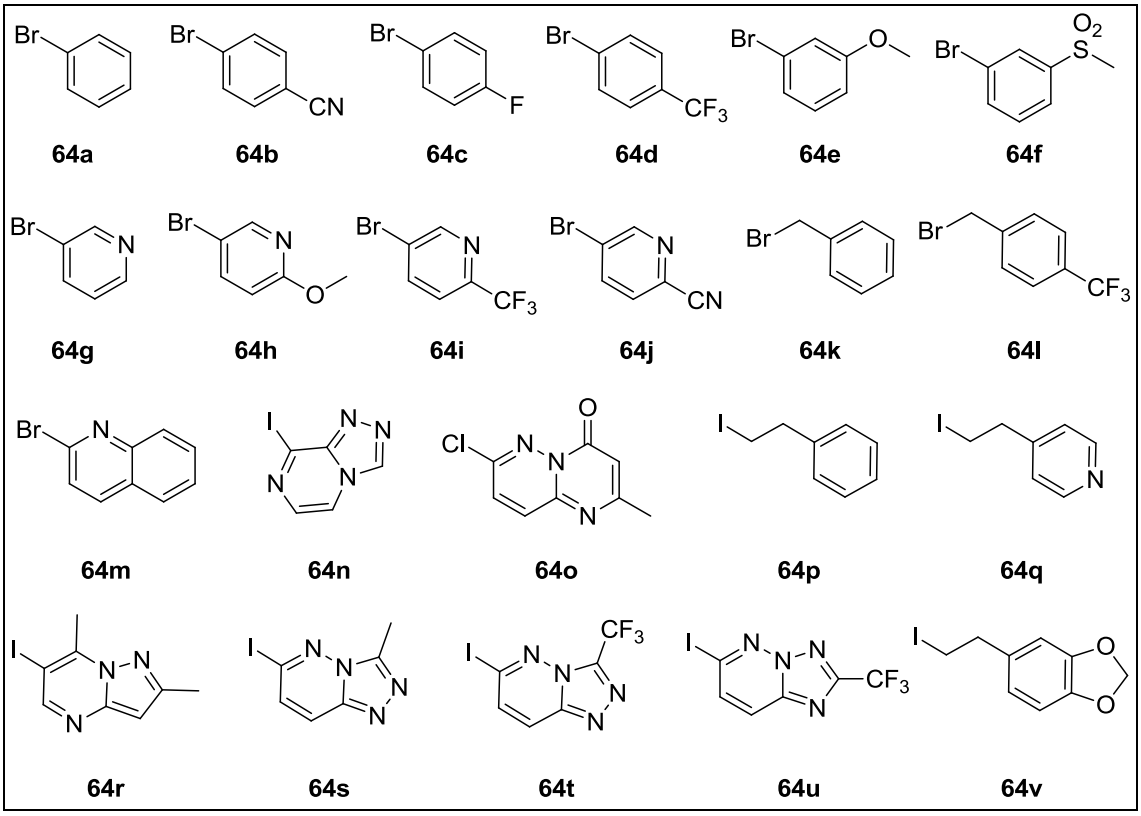

Figure 33. Structures of halo-heterocycles and halo-aromatics **64a-v**

As shown in **shceme-11** substituted bezaldehyde **51a** was synthesized from its difluoro benzene precursor **71** by formylation via Vilsmeier-Haack type reaction, using the method reported by Anthony David et al in good yield **[267]**. Whereas substituted

bezaldehydes **51b-c** used as starting material for the synthesis of aminomethyl-piperidones **69a-e** and **70a-e** were procured from the commercial bulk suppliers. Various halo-heterocycles or halo-aromatics **64a-v** required for the synthesis of aminomethyl-piperidones **68a-v**, **69a-e** and **70a-e** have been either synthesized by reported literature procedures by choosing the appropriate starting materials and optimizing reaction conditions or procured from the commercial suppliers **[268]**. However halo-aromatics and halo-heterocycle **64a-m** and **64p-q** were procured from the commercial bulk suppliers. Whereas halo-heterocycles **64n-o** and **64r-v** were synthesized by different synthetic methodologies reported in the literature (**Schemes 12-17**).

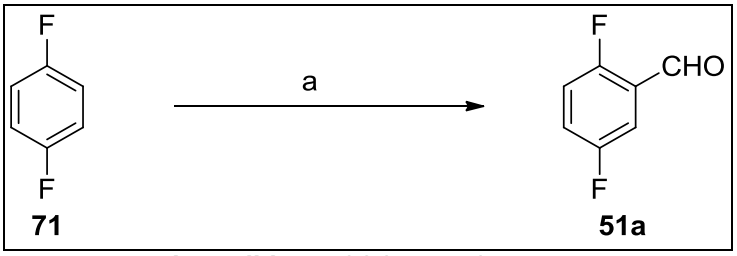

Reagents and conditions: (a) i. n-BuLi, DMF, n-Hexane, -78°C, 1h, < -65°C 1h. ii. CH_3COOH, Water, -65°C to 5°C .

Scheme 11. Synthetic method for the preparation of benzaldehyde **51a**

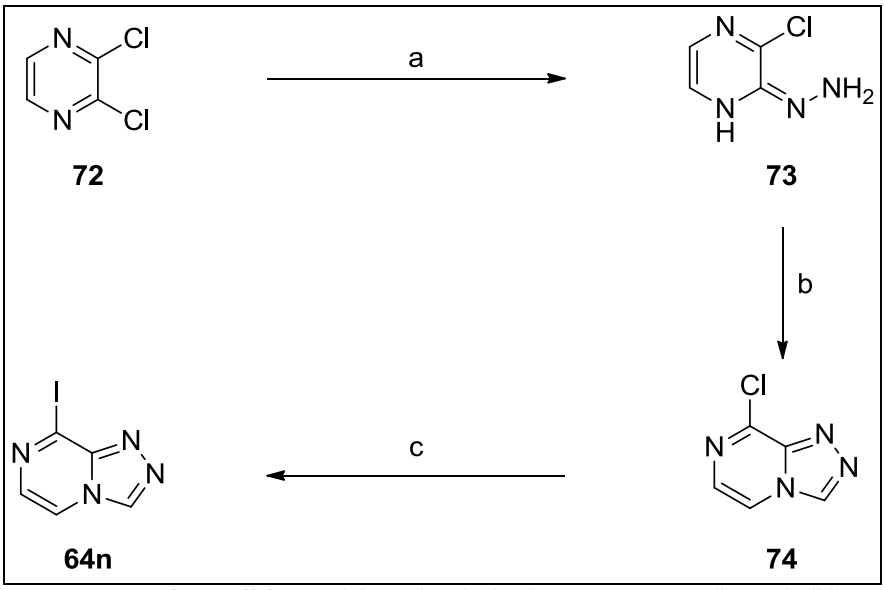

Reagents and conditions: (a) Hydrazin-hydrate, EtOH, Reflux, 2h (b) $CH(OEt)_3$, Xylene, Reflux, 4h. (c) HI, Reflux, 3days.

Scheme 12. Synthetic method for the preparation of halo-heterocycle **64n**

Heterocycle **64n** has been synthesized by various methods in the literature, here we adopted the best optimized reaction condition of each step reported in the literature for the sythesis of **64n** as outlined in **scheme 12 [31,269-271]**.

Synthesis of **64o** was carried out by making variation of a rout described by Avellana et al as illustrated in **scheme 13 [272]**.

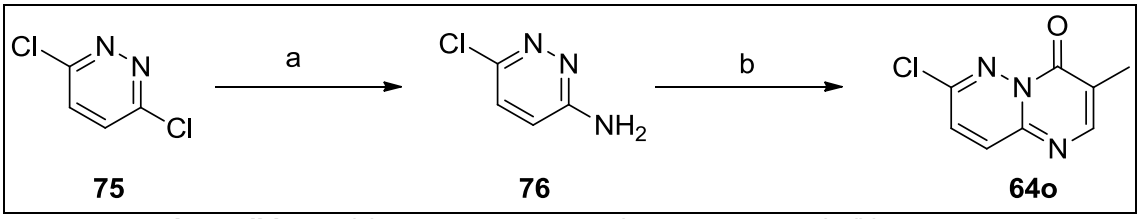

Reagents and conditions: (a) NH_4OH, 130°C, 10bar pressure, 48h (b) $CH_3COCH_2COOC_2H_5$, benzyl alcohol, Reflux, 24h.

Scheme 13. Synthetic method for the preparation of halo-heterocycle **64o**

Synthesis of **64r** (**scheme 14**) was accomplised with commercially available starting materials **77** (Which can also be prepared by method of Keisuke Suzuki et al **[273]**) and 3-Aminocrotononitrile **79** by modifying the literature procedure reported by Gerald Shipps et al and Nam et al **[274-275]**.

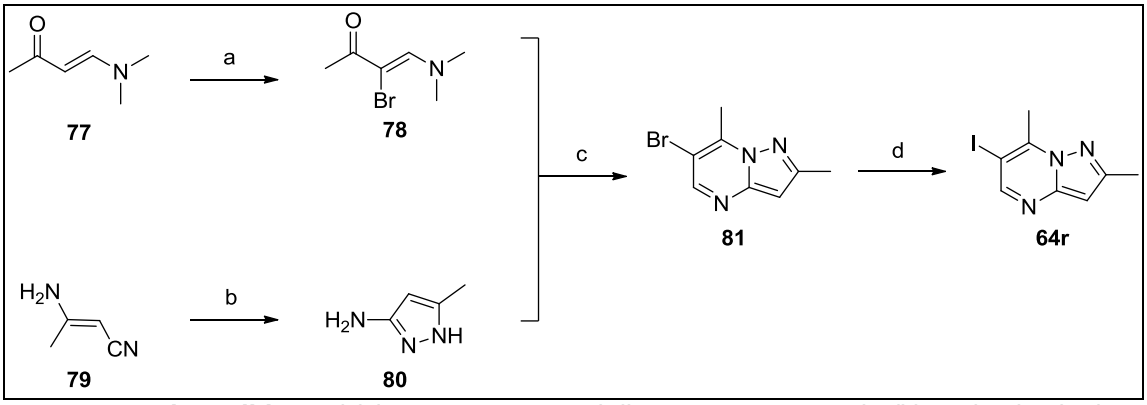

Reagents and conditions: (a) i. Br_2, DCM, 0°C, 1h ii. NEt_3, Et_2O, 0°C, 1h (b) Hydrazine hydrate, Water, Reflux, 8h (c) 33% HBr in CH_3COOH, EtOH, CH_3COOH, Reflux, 3h. (d) HI, Reflux, 3days.

Scheme 14. Synthetic method for the preparation of halo-heterocycle **64r**

Synthesis of **64s-t** was accomplished with 3,6-Dichloropyridazine **75** according to the method reported by Jason Cox et al without making any modification of reaction procedure (**scheme 15**)**[265, 271]**.

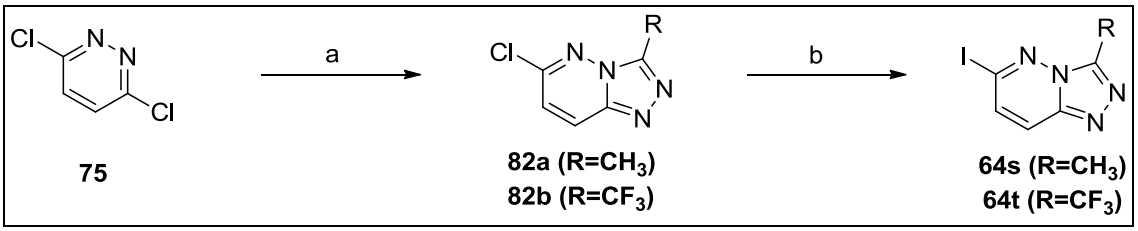

Reagents and conditions: (a) $CH_3CONHNH_2/CF_3CONHNH_2$, Butanol, Reflux, 24h. (b) HI, Reflux, 3days.

Scheme 15. Synthetic method for the preparation of halo-heterocycle **64s-t**

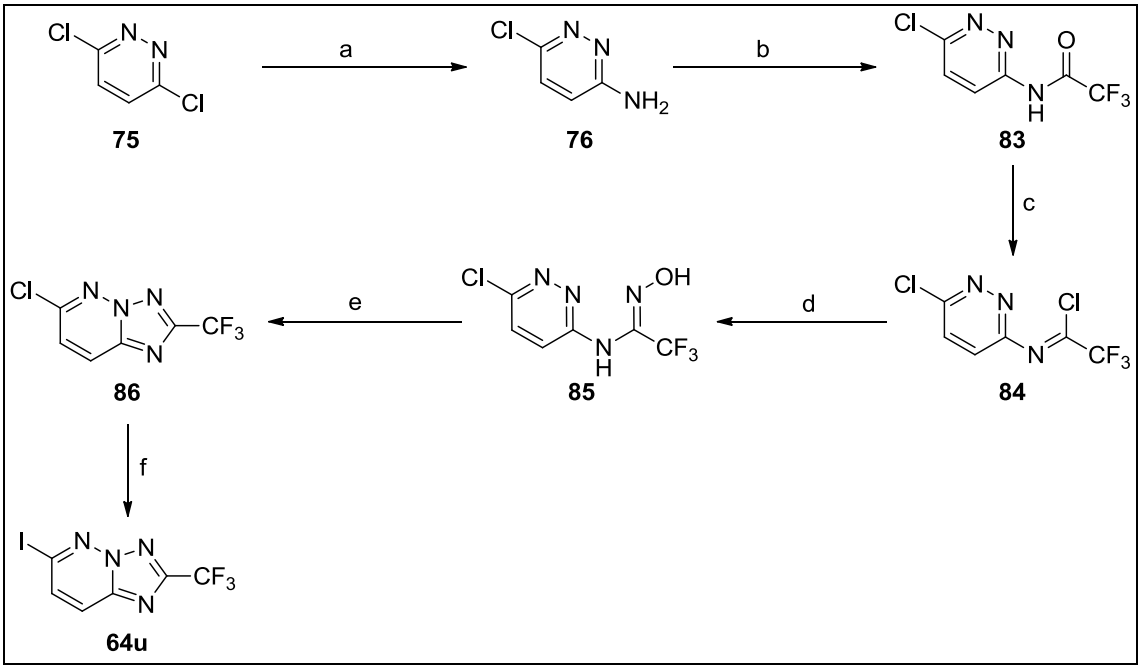

Reagents and conditions: (a) NH_4OH, 130°C, 10bar pressure, 48h (b) TFAA, NEt_3, DCM, 25°C, 24h (c) PCl_5, EDC, Reflux, 6h (d) $NH_2OH{\cdot}HCl$, 25°C, 3h (e) H_3PO_4, 150°C, 4h. (f) HI, Reflux, 3days.

Scheme 16. Synthetic method for the preparation of halo-heterocycle **64u**

For the synthesis of halo-heterocycle **64u** (**Scheme 16**), commercially available 3,6-Dichloropyridazine **75** was converted to 3-Amino-6-chloropyridazine **76** by heating with liq. ammonia under high pressure, which upon treatment with trifluoroacetic anhydride provided acyl derivative **83**. Compound **83** upon treatment with PCl_5 gave imidoylchloride **84**, which was converted to hydroxyme **85** and subsequent treatment with polyphosphoric acid provided halo-heterocycle **86**, Heterocycle **86** upon treatment with hydro iodic acid and basic workup gave desired compound **64u [265, 271]**.

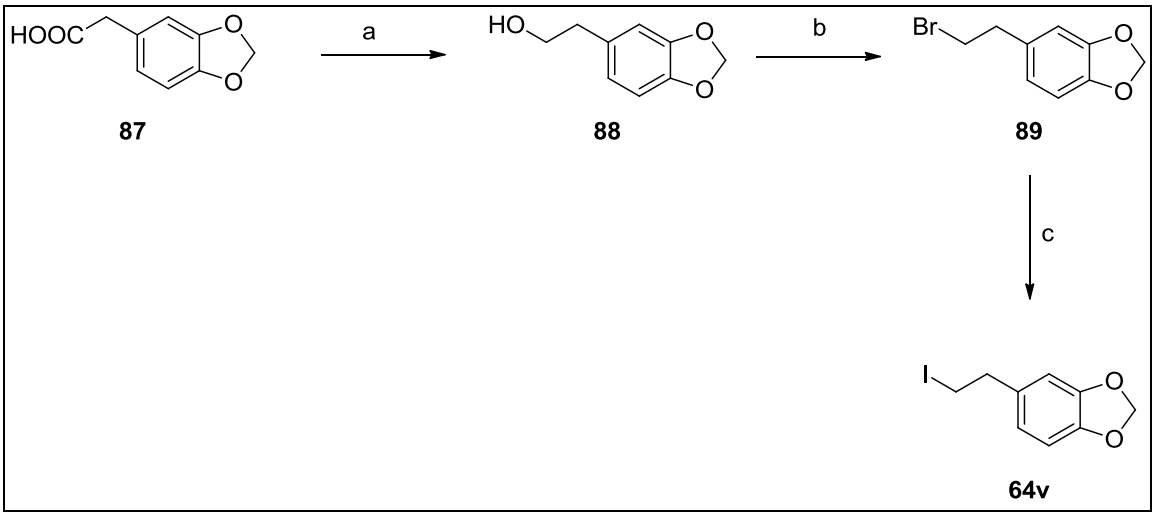

Reagents and conditions: (a) $LiAlH_4$, THF, 0°C, 1h, 25°C, 5h (b) CBr_4, PPh_3, ACN, 25°C , 15h (c) NaI, Acetone, Reflux, 24h.

Scheme 17. Synthetic method for the preparation of halo-heterocycle **64v**

Various routs are reported in the literature for the synthesis of benzo-dioxole derivative **64v [276-278]**. Here we synthesized **64v** by method as illustrated in **scheme-17** starting from commercially available benzo-dioxole acetic acid **87** (procured from Taizhou Bolon Pharmachem CO. LTD. Chaina.). Compound **87** was reduced to alcohol derivative **88** by using the method reported by Patrick Bailey et al by optimizing the reaction condition **[277]**. Further compound **88** was converted to benzo-dioxole derivative **64v** through its corresponding halo derivative **89** using the method reported by Saurabh Shahane et al by modifying the reaction conditions **[278]**.

3.3.2. *In vitro* DPP-IV inhibitory activity, selectivity and structure activity relationship (SAR)

The *in vitro* DPP-IV inhibitory activity was determined in order to establish the structure-activity relationship (SAR) using fluorescence-based assay (details experimental protocol is given in **experimental Section 5.2.1.**) **[242]**. Three sets of the aminomethyl-piperidones (**68a-v**, **69a-e** and **70a-e**) were prepared (**Table 12**). In the first set (Ar = 2,5-difluoro phenyl), 22 compounds (**68a-v**) were prepared by coupling 2,5-difluoro phenyl-aminopiperidone (**63a**) with various halo-heterocycles/halo-aromatics. In the second set (Ar = 2,4,5-trifluoro phenyl), 5 compounds (**69a-e**) were prepared by replacing 2,5-difluoro phenyl with 2,4,5-trifluoro phenyl, while in third set (Ar = 2,4-

dichloro phenyl), 5 compounds (**70a-e**) were prepared by replacing 2,5-difluoro phenyl with 2,4-dichloro phenyl. All the test compounds showed varying degrees of DPP-IV inhibitory activity (IC_{50}), depending on the nature of the substituents.

Within the first set (**68a-v**), test compounds showed diverse DPP-IV inhibitory activity depending on the nature of substituents on piperidone ring system. Compounds with electron withdrawing groups (**68b**: -CN, **68c**: -F and **68d**: -CF_3) at *para*-position of phenyl ring system showed improved DPP-IV inhibitory activity, compared to unsubstituted derivative (R=-Ph; **68a**). Compounds with electron donating groups (**68e**: -OMe and **68f**: -SO_2-Me) at *para*-position of phenyl ring showed further improvement in *in vitro* DPP-IV inhibitory activity.

Replacement of phenyl ring system with 3-pyridyl (**68g**) and further substitutions with electron donating (**68h**) and withdrawing (**68i** and **68j**) groups at para-position showed moderate DPP-IV inhibitory activity. Replacement of phenyl ring system with quinoline (**68m**), triazolo[4,3-a]pyrazine (**68n**), 2-methyl-pyrimido[1,2-b]pyridazinone (**68o**), benzyl (**68k**) and further substitutions with electron withdrawing (**68l**) groups at *para*-position showed moderate DPP-IV inhibitory activity. Substitutions with ethylbenzene (**68p**), ethylpyridine (**68q**), dimethylpyrazolo[1,5-a]-pyrimidine (**68r**), 3-methyl-triazolo[4,3-b]pyridazine (**68s**), 3-trifluoromethyl-triazolo[4,3-b]pyridazine (**68t**) and 2-trifluoromethyl-triazolo[1,5-b]pyridazine (**66u**) showed good DPP-IV inhibitory activity, while **68v** (methylenedioxy phenethyl) showed superior DPP-IV inhibitory activity (IC_{50}: 8.5±0.4 nM), compared to Sitagliptin (IC_{50}: 18±2.4 nM).

In the second set (**69a-e**, Ar = 2,4,5-trifluoro phenyl), all the five compounds showed good activity, but compared to 2,5-difluoro phenyl series (Set-1 analogs, **68q**, **68r**, **68t**, **68u** and **68v**), *in vitro* DPP-IV inhibition were found to be bit weaker, while in set three (**70a**-**e**, Ar = 2,4-dichloro phenyl), *in vitro* DPP-IV inhibition were found to be slight weaker than set-1 and set-2 corresponding analogs. Thus the nature and position of halogen atom on aromatic ring system contributed significantly towards *in vitro* DPP-IV inhibition.

Further the activity difference of the corresponding analogues in all three series compounds could be due to difference in the binding inter action of the aromatic rings in S1 pocket of the DPP-IV enzyme. 2,5-difluoro phenyl might be best fitting in the S1 pocket compared to the 2,4,5-trifluoro phenyl , which could be further binding batter than 2,4-dichloro phenyl ring.

Table-12: *In-vitro* DPP-IV inhibitory activity of aminomethyl-piperidones (**68a-v**, **69a-e** & **70a-e**).

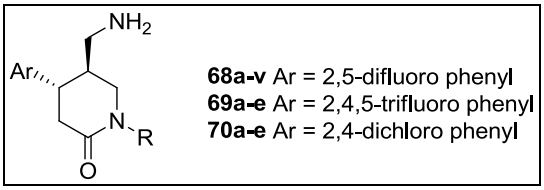

68a-v Ar = 2,5-difluoro phenyl
69a-e Ar = 2,4,5-trifluoro phenyl
70a-e Ar = 2,4-dichloro phenyl

Comp.	R	IC_{50} (nM)*	Comp.	R	IC_{50} (nM)*	Comp.	R	IC_{50} (nM)*
68a		1436±12	**68l**	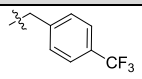	910±3.1	**69a**	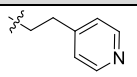	157±4.1
68b	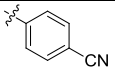	378±1.4	**68m**	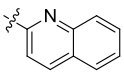	1034±21	**69b**	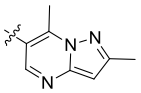	119±1.0
68c	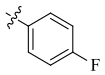	382±4.5	**68n**	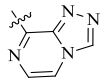	1023±3.1	**69c**	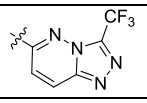	125±2.7
68d	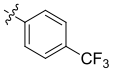	342±3.3	**68o**	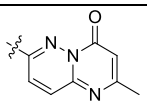	997±13.5	**69d**	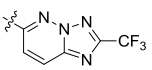	111±2.1
68e	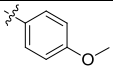	217±8.6	**68p**	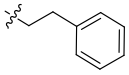	119±4.2	**69e**	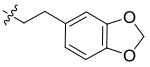	19±5.1
68f	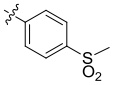	193±8.4	**68q**	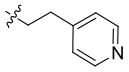	**84±2.6**	**70a**	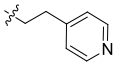	197±4.2
68g		1388±5.9	**68r**	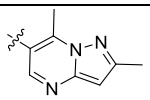	**77.6±1.2**	**70b**	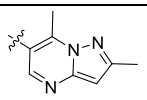	148±3.7
68h	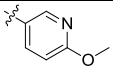	452±3.7	**68s**	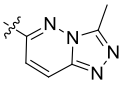	122±3.2	**70c**	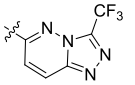	134±7.3
68i	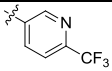	443±5.3	**68t**	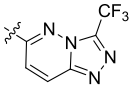	**79±0.2**	**70d**	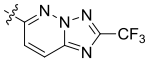	137±9.6
68j	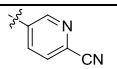	404±7.7	**68u**	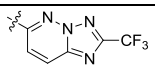	**74±0.9**	**70e**	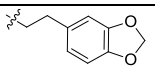	43±3.2
68k	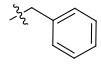	885±11.2	**68v**	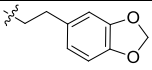	**8.5±0.4**	**Sitagliptin**	--	18±2.4

*DPP-IV inhibitory activity determined by fluorescence-based assay; fluorescence measured using Spectra Max fluorometer (Molecular Devices, CA) by exciting at 380 nm and emission at 460 nm. IC_{50} determined using Graph Pad prism software

** DPP-IV inhibitory activity represented as IC_{50} (nM), expressed as the mean ±SD (n = 3)

Overall 32 compounds screened for *in vitro* DPP-IV inhibition and here we identified compound **68v** as the most potent molecule among all the three series. Further, *in vitro* selectivity over other related serine protease, especially DPP-2, DPP-8 and DPP-9 was evaluated for **68v** and it showed >5000-fold selectivity over DPP-2 and >10,000-fold selectivity over DPP-8 and DPP-9 **[242]**.

3.3.3. *In vitro* CYP inhibition study of aminomethyl-pipyridone 68v.

To assess the CYP liabilities, **68v** was subjected for CYP1A2, CYP2C8, CYP2C9, CYP2D6, CYP2C19 and CYP3A4 inhibition studies (@1, 10 and 100 μM concentrations) and the test compound **68v** was found to be devoid of CYP1A2, CYP2C8, CYP2C9, CYP2D6, CYP2C19 and CYP3A4 inhibition up to 100 μM concentrations (details experimental protocol is given in **experimental Section 5.2.2.**).

3.3.4. *In vivo* antidiabetic activity of aminomethyl-pipyridone 68v.

Detailed pharmacodynamic (PD) profiling of **68v** was carried out. The *in vivo* antidiabetic activity of **68v** and Sitagliptin (@ 3 mg/kg, po) was evaluated in male C57BL/6J mice, using OGTT (oral glucose tolerance test) protocol (details experimental protocol is given in **experimental Section 5.2.3.**) and changes in serum glucose levels (AUC glucose up to 240 min; mg/dL) was estimated (**Figure 34**) **[243-244]**.

Compound **68v** showed good oral antidiabetic activity (% decrease in AUC glucose 38.9 ± 5.20), which was found to be better than Sitagliptin (% decrease in AUC glucose 17.9 ± 4.58). In C57 mice, it was interesting to observe that **68v** showed suppression in the blood glucose at all the time points (15, 30, 60, 120 and 240 min) compared to vehicle control, while sitagliptin showed blood glucose reduction only at 30 and 60 min.

Here this study reviles that compound **68v** might have a tendency of sustained release. Hence to understand its duration of action a separate study has been conducted in fed db/db mice for antidiabetic activity followed by pharmacokinetic (PK) study.

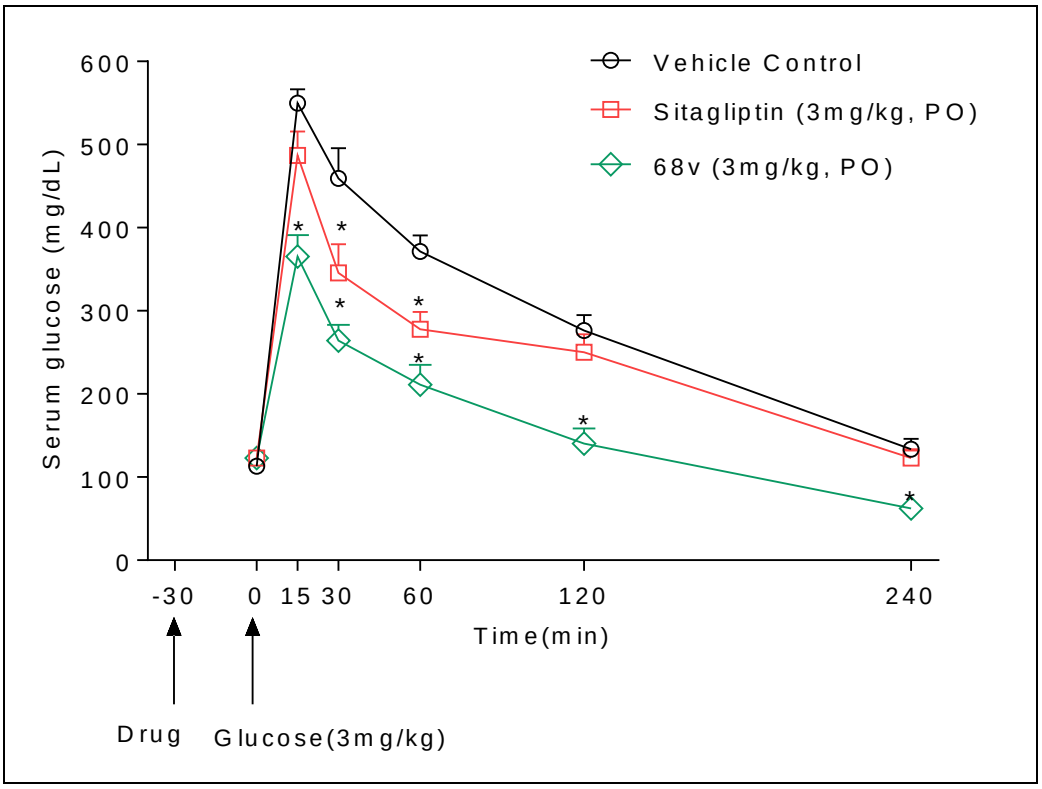

*P<0.05, Two-Way ANOVA followed by Bonferroni posttest, Mean ± SEM

Figure 34: *In vivo* antidiabetic activity of **68v** and Sitagliptin in C57 mice (OGTT)

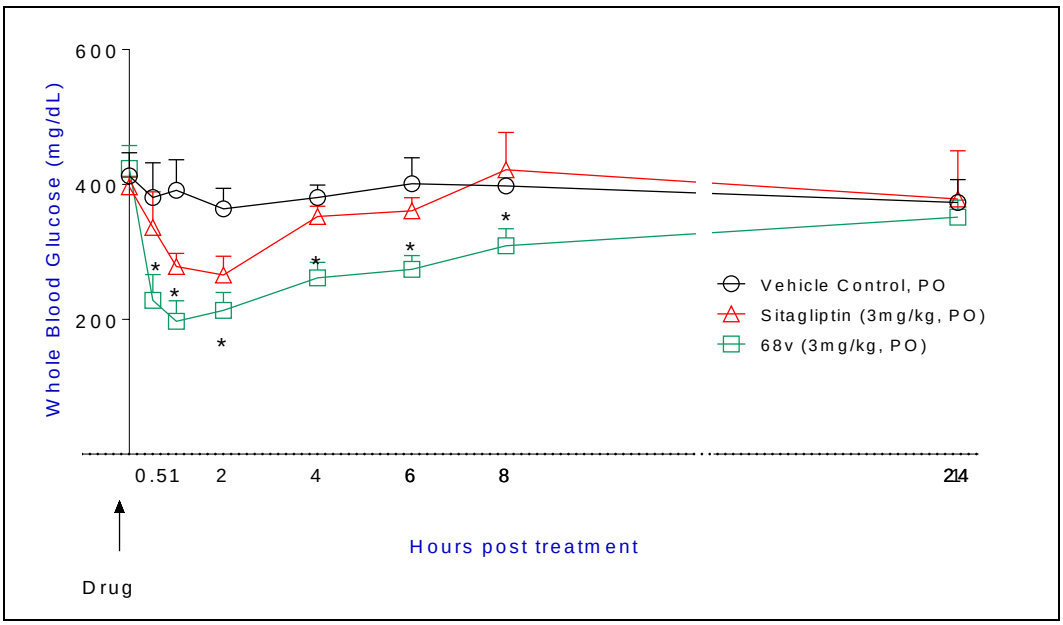

*P<0.05, Two-Way ANOVA followed by Bonferroni post test, M ± SEM

Figure 35: In vivo antidiabetic activity of **68v** and Sitagliptin in db/db mice

Further to understand the duration of action and effect of **68v** on post-prandial glucose excursion, single dose (@ 3 mg/kg, po) antidiabetic activity of **68v** and sitagliptin was evaluated in fed-db/db mice (hyperglycemic animals) for 24 h (**Figure 35**). Under fed condition, compared to vehicle control, **68v** and sitagliptin showed good antidiabetic activity (% decrease in AUC glucose 38.29 ± 12.13 and 20.80 ± 11.06, respectively) up to 2 h. However, **68v** showed prolonged suppression of serum glucose levels (% decrease in AUC glucose 20.62 ± 7.05 for **68v** and 1.48 ± 11.84 for sitagliptin, up to 24 h).

3.3.5. Pharmacokinetic (PK) studies of aminomethyl-pipyridone 68v.

A comparative single dose (3 mg/kg iv or po) PK profile of **68v** and Sitagliptin was evaluated in male C57BL/6J mice (n = 6) and the various PK parameters (T_{max}, $T_{1/2}$, C_{max}, AUC and %F) were recorded (**Table 13**) (details experimental protocol is given in **experimental Section 5.3**).

In PK study, **68v** showed rapid Tmax, higher AUC (~twofold compared to sitagliptin), extended half-life ($T_{1/2}$: >8 h) compared to sitagliptin and good oral bioavailability (%F:79.5%). Compound **68v** showed extended half-life and higher AUC, which could be due to its low clearance compared to sitagliptin (elimination rate constant (kel; h^{-1}), 0.12 ± 0.02 for **68v** and 0.84 ± 0.14 for sitagliptin). Thus improved pharmacokinetic profile of compound **68v** justifies its potent and prolonged antidiabetic activity in C57 and db/db mice.

Table 13: Pharmacokinetic study parameters[a] of **68v** and **Sitagliptin**

Compd	Tmax (h)	Cmax (mg/ml)	$T_{1/2}$ (h)	AUC (0-α) h mg/ml	%F*
68v	0.28 ± 0.12	0.42 ± 0.03	8.99 ± 0.31	1.07 ± 0.09	79.5%
Sitagliptin	0.31 ± 0.10	0.31 ± 0.01	1.56 ± 0.11	0.56 ± 0.02	75.9%

[a]In male C57BL/6J mice (n=6), compounds were administered orally (p.o) at 2 mg/kg dose and plasma concentration was analyzed by LC-MS, values indicate Mean ± SD.
* Oral bioavailability (%F) was calculated wrt to iv AUC (**68v**: 1.19 ± 0.08 & sitagliptin: 0.66 ± 0.09 h µg/ml) administered at 2 mg/kg dose, iv.

3.3.6. Molecular docking study of aminomethyl-pipyridone 68v

The molecular docking analysis of **68v** and sitagliptin, in the binding pocket of DPP-IV was carried out using extra precision (XP) Glide docking method (**Figure 36**) (details experimental protocol is given in **experimental section 5.4.**) **[245-246]**. The X-ray structure of the DPP-IV enzyme (PDB ID: 2OQI) was obtained from the protein data bank and the protein structure was prepared using protein preparation wizard module of Schrödinger. For docking study, the ligands were geometrically optimized and prepared by using ligprep module of Schrödinger.

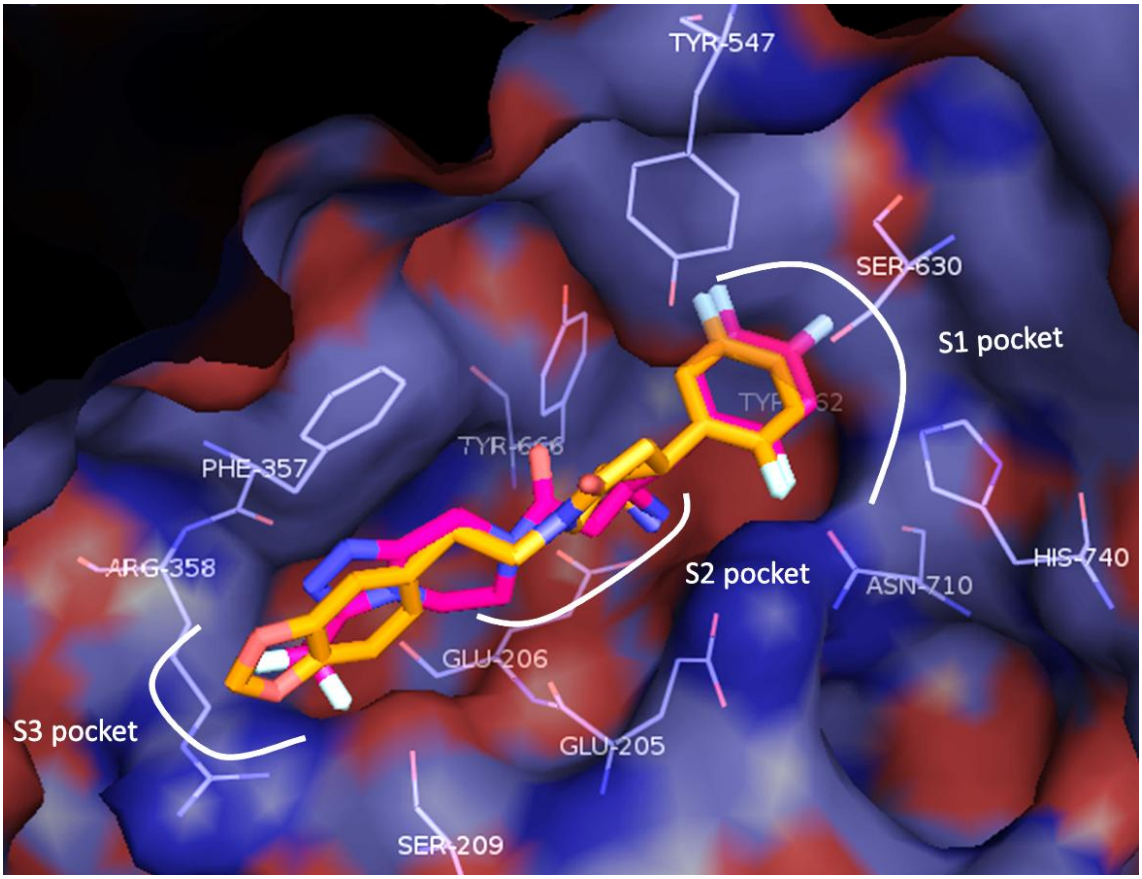

Binding pose of compound **68v** (Orange) and **Sitagliptin** (Maroon) in the DPP-IV active site is indicated (Surface view: Blue), wherein both compounds interact closely with key residues of site S_1, S_2 and S_3.

Figure 36: Key interactions of compound **68v** and Sitagliptin with active sites of DPP-IV enzyme

The overlay of binding poses of **68v** (Orange) and Sitagliptin (Maroon) in the DPP-IV active site is shown in **Figure 36**. As observed with sitagliptin, **68v** docks very well into all the three sites (G-scores -11.81 (9/9) and -10.99 (9/9) for **68v** and sitagliptin respectively). Although, G-score of **68v** and sitagliptin are comparable, however, *in vitro*, DPP-IV IC_{50} of **68v** is half of that of sitagliptin, which could be due to favorable interactions of **68v**, in all the three binding pockets. Di-fluoro-phenyl ring of **68v** occupies S1 pocket. In S2 pocket, aminomethyl groups of piperidone ring forms H-bonding with the side-chains of Glu205 and Glu206 dyad, while methylenedioxy phenyl ring of **68v** accommodates very well in S3 pocket, which together supports excellent *in vitro* DPP-IV activity and selectivity of **68v** over other protease.

3.3.7. Conclusion

Various gliptins, currently used in the clinic (Sitagliptin, Vildagliptin, Saxagliptin, Alogliptin and Linagliptin), exhibit short half-life thereby requires once or twice daily drug administration **[279-280]**. Further to regulate the pre- and post-prandial blood glucose and thereby to control HbA1c, several long-acting DPP-IV inhibitors (Omarigliptin and Trelagliptin) are under developments, as once-weekly drugs **[205]**. Their clinical efficacy and side effects profile appear to be comparable with other gliptins in the class, however, their infrequent dosing creates a niche and promotes patients compliance. In this context, overall pre-clinical profile of **68v** demonstrated added advantages over currently practiced gliptins and appears to serve as long-acting DPP-IV inhibitors.

Here we report discovery of novel aminomethyl-piperidone derivatives as potent, selective and long acting DPP-IV inhibitors for the treatment of T2DM. The lead compound **68v** ((4S,5S)-5-(aminomethyl)-1-(2-(benzo[d] [1,3]dioxol-5-yl)ethyl)-4-(2,5-difluorophenyl)-piperidin-2-one) showed prolonged suppression of pre-and post-prandial blood glucose levels (*in vivo*), which correlates with its extended PK profile.